# Center for Economic Institutions
# Working Paper Series

**No. 2023-8**


## “ Remotely measuring rural economic activity and poverty: Do we just need better sensors?”


**John Gibson, Xiaoxuan Zhang, Albert Park, Yi Jiang, and Xi Li**



**March, 2024**

Center for Economic Institutions
Working Paper Series



Institute of Economic Research
Hitotsubashi University
2-1 Naka, Kunitachi, Tokyo, 186-8603 JAPAN
https://cei.ier.hit-u.ac.jp/English/index.html
Tel:+81-42-580-8405/Fax:+81-42-580-8333

# Remotely measuring rural economic activity and poverty: Do we just need better sensors?

John Gibson (University of Waikato)[1]

Xiaoxuan Zhang (University of Waikato)

Albert Park (Asian Development Bank)

Yi Jiang (Asian Development Bank)

Xi Li (Wuhan University)

**Extended Abstract**

It is difficult and expensive to measure rural economic activity and poverty in developing countries. The usual survey-based approach is less informative than often realized due to combined effects of the clustered samples dictated by survey logistics and the spatial autocorrelation in rural livelihoods. Administrative data, like sub-national GDP for lower level spatial units, are often unavailable and the informality and seasonality of many rural activities raises doubts about accuracy of such measures. A recent literature argues that high-resolution satellite imagery can overcome these barriers to the measurement of rural economic activity and rural living standards and poverty. Potential advantages of satellite data include greater comparability between countries irrespective of their varying levels of statistical capacity, cheaper and more timely data availability, and the possibility of extending estimates to spatial units below the level at which GDP data or survey data are reported. While there are many types of remote sensing data, economists have particularly seized upon satellite-detected nighttime lights (NTL) as a proxy for local economic activity. Yet there are growing doubts about the universal usefulness of this proxy, with recent evidence suggesting that NTL data are a poor proxy in low-density rural areas of developing countries. This study examines performance in predicting rural sector economic activity and poverty in China with different types of satellite-detected NTL data that come from three generations of sensors of varying resolution. We include the most popular NTL source in economics, the Defense Meteorological Satellite Program data, whose resolution is, at best, 2.7 km, two data sources from the Visible Infrared Imaging Radiometer Suite (VIIRS) on the Suomi/NPP satellite with spatial resolution of 0.74 km, and data from the Luojia-01 satellite that is even more spatially precise, with resolution of 0.13 km. The sensors also vary in ability to detect feeble light and in the time of night that they observe the earth. With this variation we can ascertain whether better sensors lead to better predictions. We supplement this statistical assessment with a set of ground-truthing exercises. Overall, our study may help to inform decisions about future data directions for studying rural economic activity and poverty in developing countries.

[1] Corresponding author. Contact details: jkgibson@waikato.ac.nz, Department of Economics, University of Waikato, Private Bag 3105, Hamilton 3240, New Zealand. We are grateful to helpful comments from audiences at the Hitotsubashi Summer Institute, and the AARES and AEDC conferences and from seminar audiences at the University of Otago and the University of Tokyo. We especially thank the Institute of Economic Research at Hitotsubashi University for hospitality during the key stages of this research.

# I. Introduction

It is costly and difficult to measure rural economic activity and poverty in developing countries. Survey-based approaches are less informative than often realized; rural livelihoods have a high degree of spatial autocorrelation (Gibson et al, 2011) and the costs of getting interviewers into rural areas makes clustered sampling the most practical approach. Thus rural economic survey data have more uncertainty than would be found in a simple random sample of similar size that was fielded on a population whose livelihoods correlate less strongly with their neighbors (Gibson, 2019). In addition to imprecision, survey-based approaches often lack consistency in methods over time and space (DeWeerdt et al, 2020) and measurement errors can be large, especially in (self-)reported agricultural production data (Jerven and Johnston, 2015). These survey errors can spill over into national accounts data on rural sector activity, which also face other measurement constraints in developing countries (Angrist et al, 2021).

Recently it has been argued that high-resolution satellite imagery can help to overcome difficulties in measuring rural economic activity, living standards and poverty (Jean et al, 2016; Watmough et al, 2019; Lobell et al, 2020; Yeh et al, 2020). Potential advantages of remote sensing approaches include greater comparability between countries irrespective of their varying levels of statistical capacity, lower cost, the availability of higher frequency data that arrive sooner, and the possibility of building up from the pixel level to form estimates for spatial units below the level at which national accounts data or survey data are typically reported.[2] For example, Burke et al (2022) suggest that a single satellite image might be able to tell the story of a village's economic health.

There are many types of remote sensing data but economists have especially focused on satellite-detected night-time lights (NTL) as an indicator of economic activity (Chen and

[2] Survey-to-census imputation methods (e.g. Elbers et al, 2003) can facilitate construction of small-area welfare estimates (which have extended beyond expenditures and poverty to include things like food security indicators, as in Hossain et al, 2020) but the temporal coverage is usually limited by census infrequency.

Nordhaus, 2011; Henderson et al, 2012; Gibson et al, 2020). For example, Burke et al (2022) suggest that researchers can use satellite-detected data on a village's use of lights at night to draw inferences about village-level economic productivity; this is a far more granular level of analysis than would be traditionally possible. Yet there are emerging doubts about the universal usefulness of NTL data as a proxy. A study of variation in economic activity over space (but not over time) found that NTL data are a poor proxy in low-density rural areas of developing countries (Gibson et al, 2021). Relatedly, a cross-country panel study found that changes in NTL data did not positively correlate with changes in GDP in countries where agriculture and forestry were large components of GDP (Keola et al, 2015). A failure of luminosity changes to predict changes in economic activity indicators, such as employment and household spending, is also seen at local levels in developing countries (Goldblatt et al, 2020; Asher et al, 2021).

These patterns may reflect the fact that rural economic activity relies less on night-time lights than does urban sector activity. If so, finding that NTL data are less useful as a proxy for rural economic activity should hold throughout the development spectrum. Indeed, Gibson and Boe-Gibson (2021) find no relationship between changes in county-level agricultural GDP and changes in NTL data in the United States, even as activity changes in other sectors significantly correlate with changes in lights. Likewise, the cross-sectional lights-GDP relationship for the primary sector is less than one-fifth as strong as for other sectors of the US economy. The GDP data for the United States should be quite reliable so these differences in the strength of the lights-GDP relationships suggest that something about agriculture makes it less amenable to being remotely measured with NTL data.[3]

An alternative hypothesis is that because the most popular NTL data are from sensors originally designed to detect clouds for Air Force weather forecasts, failure to accurately detect

[3] Khachiyan et al (2022) use daytime imagery (from Landsat) to predict income and population for micro-grids with far greater accuracy than they achieve when using DMSP NTL data. However, their study is restricted to urbanized US census blocks and does not use modern NTL data that are more accurate (Gibson et al, 2020) and so it remains an open question as to whether rural economic activity is also hard to proxy with daytime imagery.

dimly-lit and dispersed rural economic activity should be no surprise, even if brightly-lit cities are serendipitously detected. Along these lines, Chen and Nordhaus (2015) show that data from the more accurate research-focused Visible Infrared Imaging Radiometer Suite (VIIRS) sensor reveal activity that is not detected by the widely used Defense Meteorological Satellite Program (DMSP) data; amongst 600 cells (of 1°×1°) in Africa whose populations are below 10,000, all showed light using VIIRS but 72% showed no light according to DMSP. In other words, better sensors do a better job. Thus, the failure to remotely detect rural economic activity may just be because studies have used data that rely on remote sensors that were not designed for this task.

Determining whether better sensors are all that is needed for remotely measuring rural activity and poverty, rather than it being the case that such phenomena are inherently ill-suited to remote measurement, matters to the statistics investment decisions made by developing countries and donors. Most low- and middle-income countries fund less than one-half of their national statistical plans, and rely on donors for about US$1 billion annually in funding of statistical systems (World Bank, 2021). The development of machine learning algorithms that successfully harness 'big data' is gaining considerable interest amongst development agencies even if these algorithms may yield little improvement in value-added over more traditional statistical approaches (Mahler et al, 2022). If monitoring rural economic activity and poverty is not very amenable to remote measurement approaches but such approaches get favored by new investments in statistical systems just because of their current popularity it may exacerbate an existing bias. Urban areas are relatively data-rich, even in developing countries, and NTL data are quite suitable for measuring many urban phenomena so skewing statistics investments toward remote measuring approaches may make rural areas even more relatively data poor.

The current study provides some evidence on these questions. We use satellite-detected NTL data from sensors of varying precision to predict rural economic activity and poverty in China. We use the most popular NTL data source in economics, DMSP, with spatial resolution of 2.7 km at best, two data sources from VIIRS which have spatial resolution of 0.74 km, and data from the Luojia-01 satellite whose spatial resolution is 0.13 km.[4] The ground footprints for these various sensors show the dramatic improvements in spatial precision achieved with new generations of remote sensing systems; VIIRS is a product of the 2000s and has a ground footprint that is 45-time smaller than that of DMSP, which is a product of the 1970s (Elvidge et al, 2013). In turn, Luojia-01, which launched in 2018, has a ground footprint that is 28-times smaller than that of VIIRS (and over 1500-times smaller than that of DMSP).

Another key way in which these remote sensing systems have improved is in detecting feeble lights. The Day-Night Band (DNB) sensor on VIIRS can detect lights over a range of seven orders of magnitude of radiance while DMSP detects over only two orders of magnitude so it is either top-coded in brightly lit areas (Bluhm and Krause, 2022) or it misses many dimly lit places (Chen and Nordhaus, 2015). The Luojia-01 sensor also has superior ability to detect feeble lights compared to other NTL data sources (Li et al, 2019), and this should make it very suitable for studying rural economic activity and poverty. Overall, we expect that the variation in spatial precision and in the range of luminosity conditions that can be detected by the three different remote sensing systems that we use should help to ascertain whether better sensors are sufficient to yield better predictions for rural areas.

In the next section we describe properties of the three types of NTL sensors that we use and summarize prior literature showing the superiority of Luojia-01 over VIIRS and of VIIRS over DMSP. We also report on some ground-truthing exercises we used to establish first-hand that Luojia can detect features in village areas of China that are less well detected by the other two sensors. In Section III we describe our China-wide sample of 1460 rural counties and the indicators we use when comparing predictive power of data from the NTL sensors. Our main

[4] Evidence for the ongoing popularity of DMSP data in economics comes from a Scopus search (on 27/11/23) of journal articles: outside of economics, 12% more articles published in the last two years mention VIIRS (and 'night' to rule out non-NTL uses) than mention DMSP. Yet for the economics subject area it is the other way around, with 76% more articles mentioning DMSP than VIIRS over the same two-year period.

results are in Section IV, using primary sector GDP, poverty status and fiscal revenue (all at county-level), as economic activity and welfare indicators for assessing predictions from each remote sensing system. Section V has a discussion of the broader implications of our results.

## II. The Competing Sensors

Our evaluations cover four main sources of nighttime lights (NTL) data: DSMP, two flavours of VIIRS, and Luojia-01. Table 1 has a summary of relevant attributes for the four data sources, with the top panel dealing with the satellite and sensor (just three columns are needed because the information is the same for both flavours of VIIRS data) and the bottom panel dealing with the data products.

We use the DMSP annual composites for 2018 from satellites F15 and F16.[5] These data exclude ephemeral lights from fires and flaring but there may be other forms of ephemeral light still captured in the composite. Any pixel-nights affected by clouds, moonlight, sunlight and other glare are removed at the processing stage. The observation time is ca. 3.30am, compared to the usually reported 8.30pm observation time for the DMSP time-series that ended in 2013.[6] The data are 6-bit digital numbers (DN) ranging from 0–63 (higher for more light), presented on a 30 arc-second output grid, which is roughly 0.9×0.7 km at China's latitude (but the underlying resolution of the sensor is far coarser, as discussed below).

We use VIIRS data for 2018 that are processed by two different groups in two different ways. The Earth Observation Group (EOG) at the Colorado School of Mines will be familiar to economists because the same group worked extensively on DMSP. They provide VIIRS Night Light (VNL 2.1) annual composites from monthly cloud-free radiance averages from the Suomi/NPP satellite. An initial filtering removes extraneous features such as fires and aurora

[5] These data are available from: https://eogdata.mines.edu/products/dmsp/#download
[6] Unstable orbits for DMSP satellites meant they observed the earth earlier as they aged, so Ghosh et al (2021) extended the time series past 2013 by switching from late afternoon observations, which were not useful for measuring luminosity, to the corresponding pre-dawn observations (given the 12 hour revisit time).

before the resulting rough composites have further outlier removal procedures applied (Elvidge et al, 2021). The data are in units of nano Watts per square centimetre per steradian ($nW/cm^2/sr$) on a 15 arc-second output grid (ca. 0.5×0.4 km at China's latitude). In addition to the masking of ephemeral lights there is also a stray-light correction. The second set of VIIRS data are from NASA's Black Marble collection (Román et al, 2018). The data are corrected for atmospheric, terrain, vegetation, snow, lunar, and stray light effects on radiance values, which are calibrated across time and are also validated against ground measurements. The Black Marble (BM) data differ from VNL data in four ways: reporting is with 16-bit precision (n=65,536 values) rather than 14-bit precision (n=16,384 values), the user has some control over the angle of detection, with near-nadir, off-nadir, and all-angles composites, data are given separately for snow-free and snow-covered nights, and users have to build their own composites from tiled data.[7]

The Luojia-01 satellite was developed by Wuhan University as China's first NTL sensing satellite, and was launched in June 2018. The spatial resolution is finer than any prior NTL sensor, at 130 metres, and it covers a wider range of radiance values (Li et al, 2019; Wu et al, 2021). The 14-bit digital numbers are on a 4.44 arc-second output grid (ca. 0.1×0.1 km at China's latitude). Luojia-01 better detects feeble lights than do earlier generation sensors, such as the VIIRS DNB, (Li et al., 2019a), which is likely to matter for studying rural areas. By May 2019, Luojia-01 imagery had fully covered China and some parts of Southeast Asia (Levin et al., 2020). In terms of observing economic activity, the local observation time is ca. 9.30pm, as opposed to 1.30am (BM and VNL) and 3.30am (DMSP) for the other sensors.[8]

A key attribute of these various remote sensing systems is their pixel "footprint" that is projected onto the Earth as the oscillating sensor scans a swath, of approximately 3000 km for

[7] The VNL data are available from: https://eogdata.mines.edu/nighttime_light/annual/v21/ and the Black Marble data from: https://ladsweb.modaps.eosdis.nasa.gov/achive/allData/5000/VNP46A4/. For both BM and VNL the earth observation time is ca. 1.30am.

[8] The data are available to download from the High-Resolution Earth Observation System of the Hubei Data and Application Center (http://59.175.109.173:8888/app/login.html).

DMSP, VNL and BM, and 250 km for Luojia-01 (Table 1). At nadir (the point on earth below the satellite) the lights are captured from a circular footprint but away from the nadir the angular viewing effect means that the lights are from a larger ellipse. The DMSP footprint at the nadir is approximately 25 $km^2$ (Elvidge et al, 2013); this reflects aggregation of the original ('fine') pixels into 5×5 blocks in order to conserve data storage prior to transmitting the signal to earth plus effects of geo-location errors that displace the signal by about 3 km from where the light sources are located (Tuttle et al, 2013). The footprint expands away from the nadir due to the angular viewing effect, so only images from the inner 1500 km part of the swath are used due to excessive blurring at scan extremities (Abrahams et al, 2018). Even at the half-scan point, the footprint will be about 60 $km^2$ (which is far coarser than the output grid).

In contrast to DMSP, VIIRS maintains a constant 0.55 $km^2$ footprint because the sensor compensates for effects of viewing the earth at an angle by turning off some detector elements; the spatial precision of VIIRS is also due to there being no need to aggregate pixels (there is more than adequate onboard data storage) and no geolocation errors. The Luojia-01 sensor is even more spatially precise, with a ground footprint of just 0.02 $km^2$ which is 28 times smaller than for VIIRS and 1500 times smaller than for DMSP. The relative sizes of the footprints are shown in Figure 1, which draws inspiration from a similar figure in Elvidge et al (2013) that shows why VIIRS data are superior to DMSP data for mapping nightlights.

### *2.1 Prior Literature on Performance of the Sensors*

The properties of the sensors outlined in Table 1 (especially their varying spatial precision, as shown in Figure 1) lead us to expect that the data from VIIRS should more accurately predict economic activity and poverty than does the data coming from DMSP, and likewise data from Luojia-01 should perform better than data from VIIRS. This ranking is generally borne out by the literature. For example, an early cross-sectional study found that VIIRS data are better predictors of county-level GDP in China than are DMSP data (Shi et al, 2014) and the same pattern was found at provincial and prefectural level (Dai et al, 2017). Similar comparisons have been made (cross-sectionally) for a wider set of socio-economic indicators; VIIRS data were generally a better proxy although the later observation time (compared to the pre-2014 DMSP data that observed earth in the early evening) lowered the correlations for some indicators (Jing et al, 2015).

One reason DMSP data may be predictively less accurate is outliers due to ephemeral and stray lights (Table 1). Gibson and Boe-Gibson (2021) evaluate DMSP data as a predictor of county-level GDP in the United States by comparing against two types of VIIRS data, one with outliers masked and one without masking; DMSP results are most like the ones from the unmasked VIIRS data, which suggests that the DMSP data also are affected by outliers. A feature of the DMSP measurement errors is that they are spatially mean-reverting (Gibson, 2021); hence these errors become more apparent when DMSP data are used to proxy for the economic activity of smaller, lower-level, spatial units. In contrast, aggregation to larger spatial units, such as provinces, tends to disguise the effects of the errors, because aggregation is inherently mean-reverting. Another factor that may matter is population density; China's county-level GDP is more strongly related to VIIRS data (either BM or VNL) in more densely populated areas but the DMSP data show no similar gradient (Zhang and Gibson, 2022). One reason for this lack of gradient may be from the saturation effect (top-coding) in DMSP data which make densely populated cities (which tend to be more brightly-lit) seem to be no brighter than far smaller places.

The comparisons of Luojia-01 to earlier generation sensors mostly use VIIRS data as the DMSP data for 2018 are only recently available (Ghosh et al, 2021), and 2018 is the sole year with Luojia-01 data. For example, when modelling socio-economic parameters in eastern and central regions of China, Zhang et al (2019) found that Luojia-01 data out-performed the equivalent VIIRS data. Liu et al (2020) created a 20-factor multi-dimensional economic development index for counties in three provinces (Hubei, Hunan and Jiangxi) and found that the Luojia-01 data had better fit with this index in a random forests model than did VIIRS data. Zhang et al. (2020) showed that Luojia-01 images could detect changes in lights during the 2019 Spring Festival in six cities in western China and that these changes correlate with Baidu-sourced data on short-term (holiday) migration. Lin et al (2022) found that there was a slight improvement over VIIRS when using Luojia-01 data in a random forests model for estimating the poverty status of 126 counties (and districts) in Chongqing and Guizhou in China.

### *2.2 Ground-truthing Exercises in Rural China*

To establish first-hand that Luojia-01 data capture features in rural areas of China that are less well detected by earlier generation sensors we conducted ground-truthing in three provinces (Henan, Shanxi, and Shaanxi).[9] In each province, five counties were selected for the fieldwork and two types of analyses were conducted—village transects and luminosity curves along the development spectrum.

For the transects, photographs were taken at the main crossroads in a village and then at 1 km intervals out to a 3 km perimeter. We then compared satellite-detected luminosity data for these points with what was seen on the ground. For example, in Xiyang village of Mianchi county, Henan Province, by the 3 km mark the land was devoid of buildings and was covered in crops (and an unlit pathway), at the 2km mark there were sparsely scattered building, while from the 1 km mark inwards it was all paved surfaces and built-up area, including some two storey buildings (Figure 2). The Luojia-01 data reflected this transect very closely; the highest luminosity was at the crossroads, at the 1 km mark it was 86% of that value, at the 2 km mark it was 35% of luminosity at the crossroads, and by the 3 km mark it had fallen to seven percent. The DMSP data showed no similar sensitivity; at the 3 km mark the values were still two-thirds

[9] To check if these provinces are representative we estimated elasticities of primary sector GDP with respect to luminosity from Luojia-01 using data for rural counties, province-by-province. The elasticities for these three provinces were not statistically significantly different to the elasticities for the other 24 provinces (Appendix A).

of light reported for the crossroads while at the 1 km and 2 km marks they were 88% and 80% of the value for the crossroads. Thus, DMSP data hardly distinguished the village centre from surrounding farmland. Black Marble data had a similarly flat profile, even though the VIIRS sensor has better spatial resolution than DMSP. Another example comes from Dajianbei village, Pinglu county, Shanxi Province where inability of earlier generation sensors to detect village features was even more pronounced; by 2 km from the crossroads, where there were hardly any buildings, Luojia-01 showed that luminosity had declined to just 7% of the brightest point in the village while DMSP (Black Marble) was still at 87% (79%) of the brightest value (Figure 2c, Appendix A).

For the luminosity curves we ranked each county in a province by primary sector GDP (total rather than per capita to establish where rural economies are overall more active). We then plotted GDP against total luminosity (from the various sensors) and selected five counties per province, spanning the range from low GDP to high, and visited villages in these counties to photograph the level of development seen on the ground. For example, in Taiqian county in northeast Henan we observed very sparse buildings and unpaved roads, while in Gushi, whose primary sector GDP is over seven-times higher, there were modern two-storey buildings, paved streets and vibrant activity (Figure 3). While the Luojia-01 data showed these differences, with luminosity from Gushi over twice that of Taiqian, the DMSP data had it the other way around; the poor county seemed to emit more total light than the far richer county. A likely explanation is that inherent blurring in the DMSP images seems to spread the light from brightly-lit places far and wide; Tiaqian is near big cities in Shandong (Jining and Liaocheng) and some light they emit may be wrongly attributed to Tiaqian in DMSP data.[10] Across all rural counties in Henan,

[10] Likewise, Zhongmu county in Figure 3 has a middling primary sector GDP level, at just below CNY 4 billion, yet the DMSP luminosity is almost twice as high as any other rural county in Henan (yet Luojia-01 shows nothing remarkable). Zhongmu is midway between the provincial capital Zhengzhou, with an urban population of over 10 million, and Kaifeng, with an urban population of two million, and the blurred DMSP images attribute some of the lights from these two big cities to this largely rural county.

the DMSP data provide no ability to distinguish between the poor areas and prosperous ones, with a flat trend line in Figure 3, while the Luojia-01 data do generally reflect differences seen on the ground. The differences were less marked for the two VIIRS-based data sources, which show recorded luminosity rising with primary sector GDP (Figure 1b, Appendix A) and were less marked in the other two provinces where ground-truthing fieldwork was conducted.

## III. Estimation Sample, Selected Indicators and Comparison Procedures

### *3.1 Sample*

We selected all rural counties in China to use for testing if the NTL data coming from better sensors provide more accurate predictions of rural economic activity and poverty. From all third-level sub-national units in China's 2020 census (*n*=2848) we first removed districts (these are the urban cores of cities). Next we removed county-level cities; the primary sector share of GDP in such places averages just 1.3% (and is no higher in county-level cities than in districts). This left us with a sample of n=1460. This sample is predominantly counties (n=1415) but in the parts of China that are not administered as prefectures (as the second-level unit) the other third-level units may be banners and special areas (n=45).[11] We refer to all of these as counties for simplicity. In this sample, the share of GDP from the primary sector averages 37%. The sample selection flowchart is in Appendix B, while the map showing the areas we cover is in Figure 4. The map also highlights the provinces where the ground-truthing exercises described in Section 2.2 took place.

### *3.2 Indicators of Rural Economic Activity and Welfare*

We use primary sector GDP (in billions of Yuan, CNY) for each county in 2018, from the 2019 edition of the *China Statistical Yearbook* (county-level), known in Chinese as *Zhongguo*

[11] For non-county and non-city areas (e.g. banners), if there were doubts about their suitability for inclusion the primary sector share of GDP was used as a criteria. The excluded areas were especially coal mining areas from Inner Mongolia.

*Xianyu Tongji Nianjian*.[12] The same yearbook provides our second indicator of economic activity (and of ability to fund local public goods that may affect household welfare), which is the fiscal revenue generated in each county. Our third indicator is a binary variable for the poverty status of each county, which is determined by the State Council Leading Group Office of Poverty Alleviation and Development. The basis of this classification was that a group of *n*=832 rural counties had been defined as poverty-stricken in 2013 and thereafter the National Bureau of Statistics used an annual National Rural Poverty Monitoring survey to update the progress of these counties in moving out of poverty.[13] We use the situation as it was at the beginning of 2018, when *n*=679 counties were still defined as poverty stricken across all of China, with *n*=578 of these counties in our sample.

### *3.3 Luminosity Indicators*

We use data from the competing sensors to form three sets of luminosity variables, all of which are found in applied economics studies using NTL data. The first is the sum of lights by county, which is the product of lit area and average brightness within lit areas; previous studies relating luminosity to poverty suggest this is a sufficient statistic for the relevant variation (Gibson et al, 2017; Gibson et al, 2023) and non-nested tests show that the sum of lights outperforms other luminosity variables for predicting China's county-level GDP (Zhang and Gibson, 2022). Next we use the sum of radiance divided by county area, as the way that several studies use NTL data (Henderson et al, 2012; Castelló-Climent et al, 2018) even if GDP is rarely normalized by

[12] Such disaggregated GDP data, at the third sub-national level, are rarely available; while the United States also reports county-level GDP, other large countries like India and Indonesia only report at the second sub-national (district) level, and Eurostat only reports down to the NUTS2 level, which is aggregations of counties in some countries (e.g., the UK) and provinces in others.

[13] Earlier classifications of counties as poverty stricken were found to have targeting errors with respect to per capita income (Park et al, 2002). A switch to village-level targeting (the Integrated Village Development Program) was made in 2001. This intervening regime, and the fact that the number of poverty counties in 2013 exceeded the number of poor counties from the pre-2001 regime, means that the earlier criticism of targeting errors for the pre-2001 poor county designation does not automatically apply to the post-2013 classification. In support of this claim, we show below that the current designation reflects environmental influences (such as elevation and temperature) that were previously neglected in the poor county designation (Olivia et al, 2011). Hence it is reasonable to consider this new poor county classification as a break from the past.

area. The third approach is to use the proportion of pixels in a county that are illuminated; the inverse of this measure, or relatedly the share of the population living in unlit rural areas, is used in studies of rural poverty by Smith and Wills (2018) and Maldonado (2023).

The machine learning models used in the literature to predict rural poverty often draw upon a large set of predictors and so we want to evaluate the NTL data both as unconditional predictors and also when we include covariates. For each county we have the average elevation, precipitation, and temperature, and five land cover categories—cultivated, forested, urbanized, village settlements, and industrial and infrastructural—from daytime Landsat images (Song and Deng, 2017) that we use as covariates.

For the land cover categories that refer to built-up area, there are varying relationships with luminosity that are shown by all four NTL data sources (Table 2). In particular, village settlement areas have a far smaller effect on the county sum of lights than from similarly sized urban area or industrial and infrastructural area. Averaging across the four NTL data sources, for each 1 $km^2$ of village built-up area the sum of lights is (unconditionally) 0.7 percent higher, while it is 3.8 (1.6) percent higher per 1 $km^2$ of urban (industrial and infrastructure) area. If we include all three types of built-up area in the same regression, county lights are 0.3 percent higher per $km^2$ of village area, on average and holding the other types of built-up area constant;, 2.5% higher per $km^2$ of urban area and 1.4% higher per $km^2$ of industrial and infrastructural area. For all four sources of NTL data, we would reject the hypothesis that village built-up area has the same effect on the county luminosity totals as do the other two types of built-up area. The results in Table 2 emphasize that NTL data are far more responsive to differences in urban area and in industrial and infrastructural area than they are to variations in rural areas, such as in the extent of village built-up area.

### *3.4 Empirical Specification*

We have three economic activity and welfare indicators, and these are related to the three luminosity indicators by the following regressions:

$$ln(activity\ or\ welfare\ indicator)_i = \alpha + \beta \ln(luminosity\ indicator)_i + \varepsilon_i \qquad (1)$$

where we also include control variables in some of these regressions. For one outcome (county poverty status) and for one luminosity indicator (the share of illuminated pixels) we cannot take logarithms because of the possible presence of zeros and so results in those cases use standardized variables. We place no causal interpretation on equation (1), which is just one way to find the best predictors amongst the set of NTL variables.

## IV. Results

The results of estimating equation (1) for our three outcome measures are shown in Figure 5, using the sum of lights as the luminosity indicator. Irrespective of whether we control for land cover and environmental factors, or simply look at the unconditional predictions, there is no gradient whereby the data from the more precise sensors lead to either larger elasticities of the activity or welfare indicators with respect to luminosity, or to higher $R^2$ values for the prediction equations. In other words, it does not seem that the data from newer and more precise sensors do a better job of predicting agricultural activity, poverty or fiscal revenue for these counties in rural China.[14]

In terms of each of the outcome measures, fiscal revenue is the one that is best predicted by NTL data and has the highest elasticities with respect to luminosity. While this indicator seems to show the beginning of a gradient, in the sense that the $R^2$ values and the elasticities have a ranking $BM > VNL > DMSP$ that pattern is then broken by the values for Luojia-01 being lower than for all of the other NTL data sources.[15] The predictions for primary sector

[14] In order to facilitate comparison of results across these three diverse indicators, the variables are standardized. The figures show one value for each source of NTL data (so four values), but overall we have results for seven sets of NTL data; from DMSP satellites F15 and F16 as well as their average, from VNL, from Luojia-01, and from the snow-free and weighted-average Black Marble data (BMwa). The tables report all seven results but to avoid clutter figures do not show component results, such as for DMSP F15 and F16 or for the Black Marble data that is only composed from readings on snow-free nights.

[15] Confidence intervals are not shown on the charts, to reduce clutter, but are reported in the appendix tables. For fiscal revenue and primary sector GDP the standard errors are about 0.02 and for poverty status are 0.03 in

GDP have the next highest $R^2$ values and elasticities but with little semblance of a gradient either with or without the control variables included in the specifications. For example, the $R^2$ values when using the lowest resolution DMSP data to make the predictions exceed those from two of the models using data from the more modern and spatially precise sensors (in the results with control variables included). The inability of the NTL data to predict county-level poverty status is especially clear, with none of the adjusted $R^2$ values for poverty predictions from any specification or from any NTL sensor, either with or without control variables, exceeding 0.2. In contrast, in the equations for fiscal revenue and primary sector GDP some of the $R^2$ values were approximately 0.7.

In the full results of the regressions that underpin Figure 5 (as reported in Appendix C) the lack of gradient, whereby better sensors are expected to yield data that better predict, is also seen if lights are normalized by area or if the percentage of illuminated pixels is used. For the regressions for primary sector GDP and fiscal revenue, these alternative specifications of the NTL variables are almost never as good as using the sum of lights; for example, for just two out of the 84 results in Tables 1 and 3 of Appendix C are the specifications that use variables other than the sum of lights giving the best fit. The regressions for county poverty status showed more mixed results; if land cover and the environmental controls are included then the sum of lights is generally the best fitting specification whereas if no control variables are used then lights normalized by area was generally the best fitting specification. Nevertheless, it needs to be emphasized that even with detailed earth observation data from nights (across multiple sensors) and days (using Landsat) we could not predict more than 20% of the variation in whether a county in rural China is classified as poor or not.

unconditional regressions and 0.04 with control variables. To provide a sense about the statistical significance of differences in Figure 5, one example is the unconditional elasticity of fiscal revenue with respect to luminosity; when using BM data it is four standard errors larger than the elasticity estimated using DMSP data.

### *4.1 Machine Learning Results*

The results reported thus far have used traditional regression approaches but much of the recent literature using satellite imagery for poverty predictions is based on machine learning (Hall et al, 2023). To ensure that our comparisons of the predictive power of data derived from different generations of satellite remote sensing systems are salient to this recent literature we also used a random forests (RF) algorithm (which is a form of supervised machine learning) to predict poverty. This is an ensemble learning method that combines multiple decision trees for solving classification and regression problems (Breiman, 2001). Recent studies using luminosity data in Asia find that the RF method has the highest predictive performance (Puttanapong et al, 2023; Fenz et al, 2024). A key feature for our application is that the RF method is well suited to the task of assessing variable importance, when compared to other frequently used machine learning methods (Grömping, 2015).

To obtain the RF predictions we used the randomForest package in R which allows us to have enough decision trees to generate them with randomness when building the forest. Each of the individual trees is built independently with a subset of the entire training dataset, where this subset is drawn using bootstrap sampling with replacement. Two-thirds of the instances in the bootstrap samples were used to train the individual trees, while the rest were used as testing data to evaluate the final RF classifier. The instances used for training the individual trees are referred to as in-bag instances, and the instances for testing are out-of-bag instances. In order to achieve robust results, the processing of building and selecting the final RF model is repeated 1000 times. This ensured that the RF model can include different sets of predictor variables in the training and testing samples, so that stable and reliable results are produced.

We first used just the four NTL predictors (the log of the sum of lights from DMSP, VNL, BM and Luojia-01) and then subsequently included the eight environmental factors and land cover variables as features in the ensembles of decision trees used for classifying counties as either poor or not. We use the index "%IncMSE" (the percentage increase in the mean square error) to measure the relative importance of each predictor variable. This index is constructed by randomly assigning a value to a predictor variable; for a predictor that is relatively important there will be a larger rise in the MSE (in other words, a penalty) if an actual value is replaced with a random value, compared to the case of replacing values for other variables with random values. As shown in Figure 6, the BM and DMSP data showed more importance than the other two NTL variables in the RF model without environmental variables (panel a). In other words, even using a machine learning approach, there is no appearance of a gradient whereby the data from newer and precise NTL sensors such as Luojia-01 seem to provide better predictions of rural poverty. This lack of gradient is also apparent when environmental variables are included as predictors (panel b), and the inclusion of these variables also shows that the most important variables for predicting county-level poverty in rural China appear to be elevation and temperature, rather than luminosity.

### *4.2 Heterogeneity Analysis*

The rural counties that we study vary widely in terms of their population density; the $10^{th}$ percentile is under 10 persons per $km^2$ and the $90^{th}$ percentile is 567 per $km^2$ the (median density is 131). Previous evidence for China shows that it is for the more densely populated areas that VIIRS data (from both VNL and BM) are most closely related to total GDP at county level (this evidence included urban districts, that are at an equivalent level in the administrative hierarchy), whereas the DMSP data had no such gradient with respect to density (Zhang and Gibson, 2022). To check if this same pattern holds here with our exclusively rural sample, we split the sample at the median density, with results of the prediction equations for the low density and high density counties reported in Table 3. In comparison to Figure 5 (and to the tables in Appendix C), the outcome measure now is total GDP rather than primary sector GDP and so $R^2$ values are higher just from this change (from 21% higher for VNL to 47% higher for

BM; the average rise is 36%). This is just another manifestation of the fact that agricultural activity is not very well proxied by NTL data; thus, if an outcome measure is predominantly agricultural—as is the case for primary sector GDP—there are less accurate relationships with NTL data than when the outcome measure depends less on agricultural activity, as is the case for total GDP.

For three of the four sources of NTL data—VNL is the exception—the $R^2$ values for the high density counties are higher, by an average of almost 50%, compared to the low density counties, in the regressions without control variables. In the same regressions, elasticities are also about 45% larger, on average, in the high density counties reflecting the closer fit between luminosity and economic activity in densely populated areas. This result corroborates patterns previously seen elsewhere (e.g. Gibson (2021); Gibson et al (2021)). However, the introduction of control variables changes these patterns, with generally little difference in explanatory power or in elasticities between the high density and low density counties once the controls for land cover and environmental factors are included. The correlation between population density and land cover, especially the area of a county that is urban built-up area, particularly contributes to the reduced importance of variation in the sources of the NTL data.

In terms of our main focus, there is still no apparent gradient whereby the modern, more precise, sensors are yielding NTL data that are more accurate predictors of county-level GDP, in either high density or low density areas, with or without control variables. Thus the existing finding that NTL data are a poor proxy for economic activity and welfare in low density rural areas (e.g. Gibson et al, 2021) does not appear to be an artefact from researchers relying on data from outdated, low resolution, remote sensing systems such as DMSP. Instead, the lack of improvement in the predictions, when using newer and far more precise sensors, is consistent with the hypothesis that rural activity is poorly suited to remote measuring approaches using

NTL data, even when these measurement efforts are in conjunction with the use of daytime Landsat images (such as in the Table 3 results that include control variables).

## V. Discussion and Conclusions

In our analysis of rural counties drawn from all parts of China, where we use three generations of light-detecting satellite remote sensing systems, we do not find any gradient whereby more accurate predictions of rural economic activity and poverty come from the newer, more precise, systems. Compared to the DMSP sensor, the newer systems have sensors that should better detect dim lights, which should be an advantage when studying rural areas. The newest of the sensors, Luojia-01, also has an advantage of observing in the evening rather than after midnight and so it is timed to coincide with a greater range of rural economic activities. The lack of gradient is notable because our own ground-truthing exercises showed that data from the newest and most precise sensor, Luojia-01, did capture features of the built environment in villages in these rural counties that were less well detected by the older and coarser resolution sensors. Our findings also go against the general thrust of the literature that suggests that newer sensors do a better job of predicting economic activity and poverty.

The question motivating our study is what accounts for poorer predictive performance of NTL data when used for low density rural areas, as found by Gibson et al (2021) and Zhang and Gibson (2022). A prior macro-level study also found night-time lights were a poor proxy for economic activity if agriculture and forestry are a large share of GDP (Keola et al, 2015). Are these results just arising because these studies used data from sources such as DMSP that were not designed to observe sparsely spread and dimly lit lights on earth, and so it should be no surprise that data from these older sensors are poor predictors in such settings, or is it, instead, due to the fact that most rural economic activity is inherently ill-suited to these remote measurement approaches because use of night-time lights is limited. Our results support the second hypothesis; the predominant rural activity is agriculture that rarely needs concentrated sources of light (Bluhm and McCord, 2022), so activity in this sector and the economic welfare of sector participants are ill-suited to remote measurement using light-sensing satellites. In other words, the payoffs to using newer and better NTL sensors to measure and predict rural outcomes are fairly muted (and may be zero) even if there may be a reward to using these newer sensors for studying urban areas.

In terms of differences between these findings and the published literature, the current evaluation is far more comprehensive, both over space and in terms of indicators. Prior studies for China typically compare just two sources of luminosity data, such as VIIRS and DMSP or Luojia-01 and VIIRS, and are usually for just a few provinces. In terms of the difference from our own ground-truthing exercises, which showed that Luojia-01 could pick up village features not picked up by the other sensors, the scale and spatial autocorrelation of county-level data is likely to matter. The median area of the counties we study is 2200 km$^2$ and only 12% of them are below 1000 km$^2$. At this scale, the fact that the ground footprint of Luojia-01 is 0.02 km$^2$ whereas for DMSP it is at least 25 km$^2$ provides less advantage than it might for smaller spatial units. Furthermore, there is considerable spatial autocorrelation in rural China, with statistically significant Moran's *I* statistics for primary sector GDP and poverty of 0.49 and 0.36.[16] Thus, the fact that the older and lower resolution DMSP system yields blurred data (Abrahams et al, 2018), with some lights attributed to particular counties coming from elsewhere (as discussed in Figure 3), may matter less than it would if these same data were used to study more spatially variegated indicators at a local scale. Hence, it would be useful to repeat our research in a setting where there are village-level indicators available as a benchmark, which may provide a testing ground that shows a greater payoff to spatial precision.

[16] Moran's *I* is equivalent to the slope coefficient in a linear regression of $Wz$ on $z$ where $W$ is a spatial weights matrix (Anselin, 1988). In other words, it examines the strength of the relationship between one observation and the spatially weighted average of its neighboring observations. The NTL data also show spatial autocorrelation, with Moran's *I* values of 0.41 (DMSP), 0.43 (VNL), 0.27 (BM) and 0.41 (Luojia-01). All of the *I* statistics are statistically significant at the $p$<0.01 level.

Some support for our main finding of a lack of gradient comes from a recent review of studies that use machine learning and earth observation satellite imagery to predict poverty (Hall et al, 2023). The meta-analysis based on 60 studies found that the spatial resolution of the satellite imagery was unrelated to the accuracy of the subsequent predictions made about poverty. In other words, studies using data from better sensors did not seem to do a better job of predicting poverty, which is the same pattern that we find for rural China.

A potential criticism of our findings is that some high profile remote sensing studies of poverty in developing areas concentrate on using daytime images rather than NTL data, because it is argued that very poor rural areas lack sufficient variation in night-time lights (Yeh et al, 2020; Hall et al, 2023). Yet some of these high profile studies have used transfer learning approaches that combine daytime and night-time images (e.g. Jean et al, 2016) and so they still utilize NTL data. Furthermore, some studies in economics claim to directly measure poverty with night-time lights data (or with the absence of lights), such as Smith and Wills (2018) and Maldonado (2023). This prior direct use of night-time lights data to study poverty helps make our findings salient. Moreover, given that we also use daytime Landsat images to create land cover variables we believe that our findings can be related to some of the high profile studies that used both night-time and daytime images. We therefore believe that our findings should be considered when investment decisions are made about future data directions for studying rural economic activity and poverty in developing areas.

In arguing that newer is not necessarily better, in terms of the types of data used to study poverty in rural areas of developing countries, we are not defending the *status quo* methods. While rural livelihoods will remain spatially correlated, given the use of environmental inputs, which therefore means that rural samples will be less informative than similarly-sized samples in less correlated places, there is still scope to improve the surveys.[17] For example, many rural surveys are highly clustered, with a dozen or more households surveyed per enumeration area (EA). Less clustered samples would help to increase our confidence in survey results. Such a change could be timely because recent FAO and World Bank (2018) guidelines for food data collection recommend switching to 7-day recall surveys. With this survey design, interviewers can spend less time in each EA compared to when they were required to monitor households who were filling out expenditure diaries for 14-days.[18] Evidence for this time-saving comes from a recent experiment where the same teams of interviewers switched between diary and recall formats when assigned a new workload in each survey round; with recall they had ample free time but if fielding diaries they struggled to complete their workload (Sharp et al, 2022). Hence, survey experiments where fewer households per EA are surveyed but more EAs are sampled could be fruitful, just as experiments like those of Beegle et al (2012) helped to change other aspects of survey design in developing countries.

Yet interest in such experiments may be limited by apparent success of the high profile machine learning studies using satellite remote sensing to predict rural poverty. Donors may reason that there is less need for surveys if we can rely on satellites. Our results provide grounds for caution. If rural economic activity and poverty are poorly suited to remote study, as we find, but current fashion leads to more use of satellite-based approaches, it may exacerbate an existing data inequality. Specifically, rural areas are already data poor. We showed here (in Table 2) that night-time lights are far more sensitive to urban activity than rural activity, and so further investments into remote sensing approaches may inadvertently be pro-urban even if motivated by a desire to modernize the study of rural poverty. Indeed, to the extent that future

[17] Many of the SDGs are tail-based measures, such as proportions of the population either hungry or poor, and so they depend not only on measures of means and totals (what many household economic surveys historically focused on) but also on variances (Gibson, 2020). Hence, sample efficiency matters to SDG monitoring.

[18] At the very least, interviewers for diary surveys would return each week to pick up the completed diary and distribute a new diary for the coming week. In situations with illiterate households the interviewers often needed to revisit every second day (Beegle et al, 2012).

funding for remote measurement approaches to rural poverty is at the expense of improvements in the traditional survey approaches, these investments may impair our understanding of rural poverty in the future.

## References


Abrahams, A., Oram, C., & Lozano-Gracia, N. (2018). Deblurring DMSP nighttime lights: A new method using Gaussian filters and frequencies of illumination. *Remote Sensing of Environment*, *210*, 242-258.

Angrist, N., Goldberg, P. K., & Jolliffe, D. (2021). Why is growth in developing countries so hard to measure? *Journal of Economic Perspectives*, *35*(3), 215-42.

Anselin, L. (1988). *Spatial Econometrics: Methods and Models*, Dordrecht: Kluwer Academic Publishers.

Asher, S., Lunt, T., Matsuura, R., & Novosad, P. (2021). Development research at high geographic resolution: an analysis of night-lights, firms, and poverty in India using the SHRUG open data platform. *The World Bank Economic Review*, *35*(4), 845-871.

Beegle, K., De Weerdt, J., Friedman, J., & Gibson, J. (2012). Methods of household consumption measurement through surveys: Experimental results from Tanzania. *Journal of Development Economics, 98*(1), 3-18.

Bluhm, R., & Krause, K. (2022). Top lights: Bright cities and their contribution to economic development. *Journal of Development Economics*, *157*(1), 102880.

Bluhm, R., & McCord, G. (2022). What can we learn from nighttime lights for small geographies? Measurement errors and heterogeneous elasticities. *Remote Sensing, 14*(5), 1190.

Breiman, L. (2001). Random forests. *Machine Learning*, *45*(1), 5-32.

Burke, M., Driscoll, A., Lobell, D., & Ermon, S. (2022). Using satellite imagery to understand and promote sustainable development. *HAI Policy Brief*, Stanford Institute for Human-Centered Artificial Intelligence. https://hai.stanford.edu/policy-brief-using-satellite-imagery-understand-and-promote-sustainable-development

Chen, X., & Nordhaus, W. (2011). Using luminosity data as a proxy for economic statistics. *Proceedings of the National Academy of Sciences*, *108*(21), 8589-8594.

Chen, X., & Nordhaus, W. (2015). A test of the new VIIRS lights data set: Population and economic output in Africa. *Remote Sensing*, *7*(4), 4937-4947.

Castelló-Climent, A., Chaudhary, L., & Mukhopadhyay, A. (2018). Higher education and prosperity: From Catholic missionaries to luminosity in India. *The Economic Journal*, *128*(616), 3039-3075.

Dai, Z., Hu, Y., & Zhao, G. (2017). The suitability of different nighttime light data for GDP estimation at different spatial scales and regional levels. *Sustainability*, *9*(2), 305.

De Weerdt, J., Gibson, J., & Beegle, K. (2020). What can we learn from experimenting with survey methods? *Annual Review of Resource Economics*, *12*, 431-447.

Elbers, C., Lanjouw, J., & Lanjouw, P. (2003). Micro-level estimation of poverty and inequality. *Econometrica*, *71*(1), 355-364.

Elvidge, C., Baugh, K., Zhizhin, M., & Hsu, F-C. (2013). Why VIIRS data are superior to DMSP for mapping nighttime lights. *Proceedings of the Asia-Pacific Advanced Network*, *35*(0), 62.

Elvidge, C., Zhizhin, M., Ghosh, T., Hsu, F-C., & Taneja, J. (2021). Annual time series of global VIIRS nighttime lights derived from monthly averages: 2012 to 2019. *Remote Sensing*, *13*(5), 922.

Fenz, K., Mitterling, T., Martinez, A., Bulan, J., Durante, R., Martillan, M., Addawe, M., & Roitner-Fransecky, I., (2024). Compiling granular population data using geospatial information. *Asian Development Review*, *41*(1), 1-39.

Food and Agriculture Organization of the United Nations (FAO) and the World Bank. (2018). *Food Data Collection in Household Consumption and Expenditure Surveys: Guidelines for Low-and Middle-Income Countries*. Accessed on 2 June, 2022 from: https://openknowledge.worldbank.org/handle/10986/32503. Rome & Washington D.C.: Food and Agriculture Organization (FAO) and the World Bank.

Ghosh, T., Baugh, K., Elvidge, C., Zhizhin, M., Poyda, A., & Hsu, F-C. (2021). Extending the DMSP nighttime lights time series beyond 2013. *Remote Sensing*, *13*(24), 5004.

Gibson, J. (2019). Are you estimating the right thing? An editor reflects. *Applied Economic Perspectives and Policy*, *41*(3), 329-350.

Gibson, J. (2020). Measuring chronic hunger from diet snapshots. *Economic Development and Cultural Change*, *68*(3), 813-838.

Gibson, J. (2021). Better night lights data, for longer. *Oxford Bulletin of Economics and Statistics*, *83*(3), 770-791.

Gibson, J., & Boe-Gibson, G. (2021). Nighttime lights and county-level economic activity in the United States: 2001 to 2019. *Remote Sensing*, *13*(14), 2741.

Gibson, J., Datt, G., Murgai, R., & Ravallion, M. (2017). For India's rural poor, growing towns matter more than growing cities. *World Development*, *98*, 413-429.

Gibson, J., Jiang, Y., & Susantono, B. (2023). Revisiting the role of secondary towns: How different types of urban growth relate to poverty in Indonesia. *World Development*, *169*, 106281.

Gibson, J., Kim, B., & Olivia, S. (2011). Spatial correlation in household choices in rural Indonesia. *Asian Economic Journal*, *25*(3), 271-289.

Gibson, J., Olivia, S., & Boe-Gibson, G. (2020). Night lights in economics: Sources and uses. *Journal of Economic Surveys*, *34*(5), 955-980.

Gibson, J., Olivia, S., Boe-Gibson, G., & Li, C. (2021). Which night lights data should we use in economics, and where? *Journal of Development Economics*, *149*, 102602.

Goldblatt, R., Heilmann, K., & Vaizman, Y. (2020). Can medium-resolution satellite imagery measure economic activity at small geographies? Evidence from Landsat in Vietnam. *The World Bank Economic Review*, *34*(3), 635-653.

Grömping., U. (2015). Variable importance in regression models. *Wiley Interdisciplinary Reviews: Computational Statistics, 7,* 137-152.

Hall, O., Dompae, F., Wahab, I., & Dzanku, F. M. (2023). A review of machine learning and satellite imagery for poverty prediction: Implications for development research and applications. *Journal of International Development* **https://doi.org/10.1002/jid.3751**

Henderson, V., Storeygard, A., & Weil, D. (2012). Measuring economic growth from outer space. *American Economic Review*, *102*(2), 994-1028.

Hossain, M., Das, S., Chandra, H., & Islam, M. (2020). Disaggregate level estimates and spatial mapping of food insecurity in Bangladesh by linking survey and census data. *PloS one*, *15*(4), e0230906.

Jean, N., Burke, M., Xie, M., Davis, W., Lobell, D., & Ermon, S. (2016). Combining satellite imagery and machine learning to predict poverty. *Science*, *353*(6301), 790-794.

Jerven, M., & Johnston, D. (2015). Statistical tragedy in Africa? Evaluating the data base for African economic development. *The Journal of Development Studies*, *51*(2), 111-115.

Jing, X., Shao, X., Cao, C., Fu, X., & Yan, L. (2015). Comparison between the Suomi-NPP Day-Night Band and DMSP-OLS for correlating socio-economic variables at the provincial level in China. *Remote Sensing*, *8*(1), 17.

Keola, S., Andersson, M., & Hall, O. (2015). Monitoring economic development from space: using nighttime light and land cover data to measure economic growth. *World Development*, *66*, 322-334.

Khachiyan, A., Thomas, A., Zhou, H., Hanson, G., Cloninger, A., Rosing, T., & Khandelwal, A. (2022). Using neural networks to predict micro-spatial economic growth. *American Economic Review: Insights*, *4*(4), 491-506.

Levin, N., Kyba, C. C. M., Zhang, Q., Sánchez de Miguel, A., Román, M. O., Li, X., Portnov, B. A., Molthan, A. L., Jechow, A., Miller, S. D., Wang, Z., Shrestha, R. M., & Elvidge, C. D. (2020). Remote sensing of night lights: A review and an outlook for the future. *Remote Sensing of Environment*, 237, 111443.

Li, X., Li, X., Li, D., He, X., & Jendryke, M. (2019). A preliminary investigation of Luojia-1 night-time light imagery. *Remote Sensing Letters*, *10*(6), 526-535.

Li, X., Liu, Z., Chen, X., & Sun, J. (2019). Assessing the ability of Luojia 1-01 imagery to detect feeble nighttime lights. *Sensors*, *19*(17), 3708.

Lin, J., Luo, S., & Huang, Y. (2022). Poverty estimation at the county level by combining LuoJia1-01 nighttime light data and points of interest. *Geocarto International*, *37*(12), 3590-3606.

Liu, H., Luo, N., & Hu, C. (2020). Detection of county economic development using LJ1-01 nighttime light imagery: A comparison with NPP-VIIRS data. *Sensors*, *20*(22), 6633.

Lobell, D., Azzari, G., Burke, M., Gourlay, S., Jin, Z., Kilic, T., & Murray, S. (2020). Eyes in the sky, boots on the ground: Assessing satellite-and ground-based approaches to crop yield measurement and analysis. *American Journal of Agricultural Economics*, *102*(1), 202-219.

Mahler, D., Castañeda Aguilar, R., & Newhouse, D. (2022). Nowcasting global poverty. *World Bank Economic Review*, *36*(4), 835-856.

Maldonado, L. (2023). Living in darkness: rural poverty in Venezuela. *Journal of Applied Economics*, *26*(1), 2168464.

Olivia, S., Gibson, J., Rozelle, S., Huang, J., & Deng, X. (2011). Mapping poverty in rural China: how much does the environment matter? *Environment and Development Economics*, *16*(2), 129-153.

Park, A., Wang, S., & Wu, G. (2002). Regional poverty targeting in China. *Journal of Public Economics*, *86*(1), 123-153.

Puttanapong, N., Prasertsoong, N., & Peechapat, W. (2023). Predicting provincial Gross Domestic Product using satellite data and machine learning methods: A case study of Thailand. *Asian Development Review*, *40*(2), 39-85.

Román, M., Wang, Z., Sun, Q., Kalb, V., Miller, S., Molthan, A., Schultz, L., Bell, J., Stokes, E., Pandey, B., & Seto, K. (2018). NASA's Black Marble nighttime lights product suite. *Remote Sensing of the Environment*, *210*, 113-43.

Sharp, M. K., Buffière, B., Himelein, K., Troubat, N., & Gibson, J. (2022). Effects of data collection methods on estimated household consumption and survey costs. *Policy Research Working Paper* No. 10029, The World Bank.

Shi, K., Yu, B., Huang, Y., Hu, Y., Yin, B., Chen, Z., Chen, L., & Wu, J. (2014). Evaluating the ability of NPP-VIIRS nighttime light data to estimate the gross domestic product and the electric power consumption of China at multiple scales: A comparison with DMSP-OLS data. *Remote Sensing*, *6*(2), 1705-1724.

Smith, B., & Wills, S. (2018). Left in the dark? Oil and rural poverty. *Journal of the Association of Environmental and Resource Economists*, *5*(4), 865-904.

Song, W., & Deng, X. (2017). Land-use/land-cover change and ecosystem service provision in China. *Science of the Total Environment*, *576*, 705-719.

Tuttle, B., Anderson, S., Sutton, P., Elvidge, C., & Baugh, K. (2013). It used to be dark here. *Photogrammetric Engineering & Remote Sensing*, *79*(3), 287-297.

Watmough, G., Marcinko, C., Sullivan, C., Tschirhart, K., Mutuo, P., Palm, C., & Svenning, J. (2019). Socio-ecologically informed use of remote sensing data to predict rural household poverty. *Proceedings of the National Academy of Sciences*, *116*(4), 1213-1218.

World Bank. (2021). *World Development Report 2021: Data for Better Lives.* World Bank Group, Washington DC.

Wu, J., Zhang, Z., Yang, X., & Li, X. (2021). Analyzing pixel-level relationships between Luojia 1-01 nighttime light and urban surface features by separating the pixel blooming effect. *Remote Sensing*, *13*(23), 4838.

Yeh, C., Perez, A., Driscoll, A., Azzari, G., Tang, Z., Lobell, D., Ermon, S., & Burke, M. (2020). Using publicly available satellite imagery and deep learning to understand economic well-being in Africa. *Nature Communications*, *11*(1), 2583.

Zhang, G., Guo, X., Li, D., & Jiang, B. (2019). Evaluating the potential of LJ1-01 nighttime light data for modelling socio-economic parameters. *Sensors*, *19*(6), 1465.

Zhang, C., Pei, Y., Li, J., Qin, Q., & Yue, J. (2020). Application of Luojia 1-01 nighttime images for detecting the light changes for the 2019 spring festival in western cities, China. *Remote Sensing*, *12*(9), 1416.

Zhang, X., & Gibson, J. (2022). Using multi-source nighttime lights data to proxy for county-level economic activity in China from 2012 to 2019. *Remote Sensing*, *14*(5), 1282.

**Table 1.** Attributes of the various NTL data sources and data products

| | DMSP | VNL | Black Marble | LJ1-01 |
|---|---|---|---|---|
| *Satellite/Sensor Attributes* | | | | |
| Operator | US DoD | NASA/NOAA | | Wuhan University |
| Sensor | OLS | VIIRS | | CMOS |
| Available years | 1992-2019 | 2012-present | | June 2018- March 2019 |
| Wavelength range | 500-900 nm | 500-900 nm | | 460-980 nm |
| Orbit type and height | Polar, 850 km | Polar, 827 km | | Polar, 645 km |
| Spatial resolution at nadir | 2.7 km | 742 m | | 130 m |
| Swath | 3000 km | 3000 km | | 250 km |
| Revisit time | 12 hr | 12 hr | | 3-5 days |
| Pixel saturation | Saturated | Not saturated | | Not saturated |
| On-board calibration | No | Yes | | Yes |
| *Data Products* | | | | |
| Creator of annual composites | EOG | EOG | NASA | Wuhan University |
| Tiled | No | No | Yes, 648 tiles | Yes |
| Quantization | 6-bit (n=64) | 14 bit (n=16,384) | 16 bit (n=65,536) | Digital number (DN) values |
| Masking of ephemeral light sources | No | Yes | Yes | Yes |
| Stray-light correction | No | Yes, from 2014 | Yes | Yes |
| User control over angle of detection | No | No | Yes | No |
| Treatment of snow | No | No | Yes | No |

Note: DoD is Department of Defense, OLS is Operational Linescan System, VIIRS is Visible Infrared Imaging Radiometer Suite, EOG is Earth Observation Group

Table 2: Relationships between Landsat detected built-up area and luminosity (sum of lights)

| | (1) | (2) | (3) | (4) |
|---|---|---|---|---|
| | | DMSP | | |
| Urban (towns and cities) | 0.045*** | | | 0.028*** |
| | (0.004) | | | (0.002) |
| Village residential area | | 0.008*** | | 0.004*** |
| | | (0.000) | | (0.000) |
| Industrial/infrastructural | | | 0.019*** | 0.015*** |
| | | | (0.004) | (0.001) |
| **Adjusted $R^2$** | **0.303** | **0.256** | **0.105** | **0.416** |
| | | VNL | | |
| Urban (towns and cities) | 0.037*** | | | 0.021*** |
| | (0.003) | | | (0.003) |
| Village residential area | | 0.007*** | | 0.004*** |
| | | (0.000) | | (0.000) |
| Industrial/infrastructural | | | 0.015*** | 0.013*** |
| | | | (0.003) | (0.003) |
| **Adjusted $R^2$** | **0.274** | **0.251** | **0.100** | **0.391** |
| | | Black Marble | | |
| Urban (towns and cities) | 0.041*** | | | 0.030*** |
| | (0.004) | | | (0.004) |
| Village residential area | | 0.006*** | | 0.003*** |
| | | (0.000) | | (0.000) |
| Industrial/infrastructural | | | 0.018*** | 0.015*** |
| | | | (0.004) | (0.003) |
| **Adjusted $R^2$** | **0.276** | **0.177** | **0.114** | **0.366** |
| | | Luojia-01 | | |
| Urban (towns and cities) | 0.028*** | | | 0.019*** |
| | (0.002) | | | (0.002) |
| Village residential area | | 0.005*** | | 0.002*** |
| | | (0.000) | | (0.000) |
| Industrial/infrastructural | | | 0.013*** | 0.011*** |
| | | | (0.003) | (0.002) |
| **Adjusted $R^2$** | **0.194** | **0.134** | **0.088** | **0.269** |

*Notes*: The dependent variable is county-level luminosity. Intercepts are not reported to save space. Built-up area is measured in km$^2$ and the sum of lights in logs, so coefficients are (approximately) percentage differences in luminosity per 1 km$^2$ of each type of built up area. The land use for industrial and infrastructural land includes factories, mines and quarries, airports and roads. Based on $n$=1460 counties, with robust standard errors in ( ) and ***, **, and * denoting statistical significance at 1%, 5% and 10%.

Table 3: Heterogeneity analysis: comparing predictive power of night-time lights data for total GDP in low and high density areas of China

| | No control variables | | | Controls for land cover and environmental factors | | |
|---|---|---|---|---|---|---|
| | All regions | Low density | High density | All regions | Low density | High density |
| DMSP | 0.700*** | 0.392*** | 0.586*** | 0.343*** | 0.365*** | 0.275*** |
| | (0.019) | (0.024) | (0.032) | (0.021) | (0.026) | (0.043) |
| **Adjusted $R^2$** | **0.490** | **0.265** | **0.310** | **0.745** | **0.577** | **0.527** |
| VIIRS Night Lights | 0.714*** | 0.409*** | 0.485*** | 0.347*** | 0.354*** | 0.165*** |
| | (0.018) | (0.023) | (0.034) | (0.020) | (0.024) | (0.036) |
| **Adjusted $R^2$** | **0.510** | **0.301** | **0.217** | **0.752** | **0.590** | **0.513** |
| Black Marble | 0.759*** | 0.437*** | 0.645*** | 0.374*** | 0.318*** | 0.347*** |
| | (0.017) | (0.024) | (0.029) | (0.020) | (0.024) | (0.037) |
| **Adjusted $R^2$** | **0.577** | **0.313** | **0.399** | **0.759** | **0.571** | **0.552** |
| Luojia-01 | 0.431*** | 0.255*** | 0.419*** | 0.150*** | 0.145*** | 0.124*** |
| | (0.024) | (0.024) | (0.026) | (0.016) | (0.021) | (0.027) |
| **Adjusted $R^2$** | **0.185** | **0.133** | **0.260** | **0.716** | **0.497** | **0.513** |

*Notes:* The dependent variable is the logarithm of GDP, and the independent variable is the logarithm of the sum of light. The sample is split amongst 1460 counties into the above median and below median population density sub-samples. The low-density and high-density subsamples have 731, and 729 observations, respectively. Robust standard errors in ( ), $^{***}$, $^{**}$, and $^{*}$ denote statistical significance at 1%, 5% and 10% levels. The control variables in columns (4) to (6) are elevation, precipitation, temperature, and five land cover classes (three types of urban land, cultivated land, and forest).

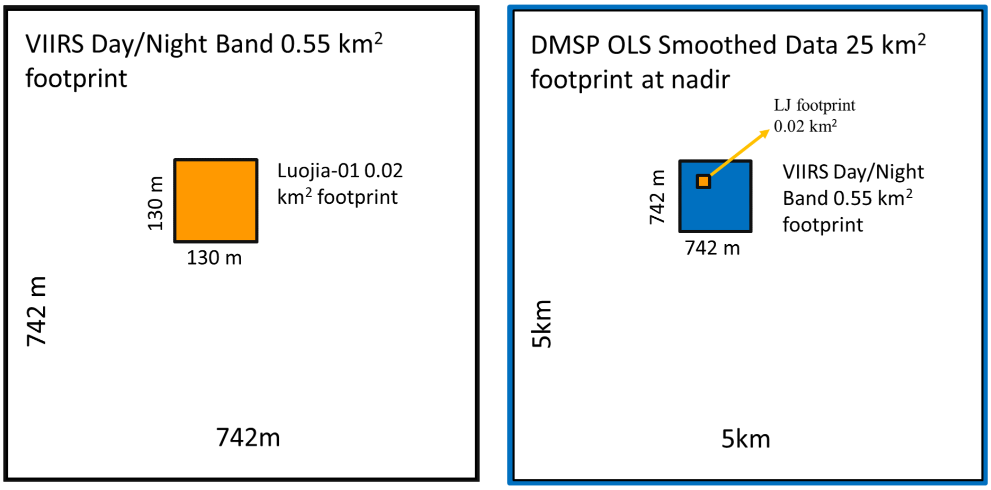


(a) Luojia-01 (LJ) versus VIIRS (VNL and BM) (b) LJ versus VIIRS versus DMSP

Figure 1. The DMSP-OLS nighttime visible band are collected with a 5 km × 5 km footprint (after on-board averaging), VIIRS DNB data, are collected with a 742 m × 742 m pixel footprint from nadir out to the edge of scan, and Luojia-01 (LJ) nighttime data has a 130 m × 130 m footprint. (*After:* Elvidge et al (2013) "Why VIIRS data are superior to DMSP for mapping night time lights").

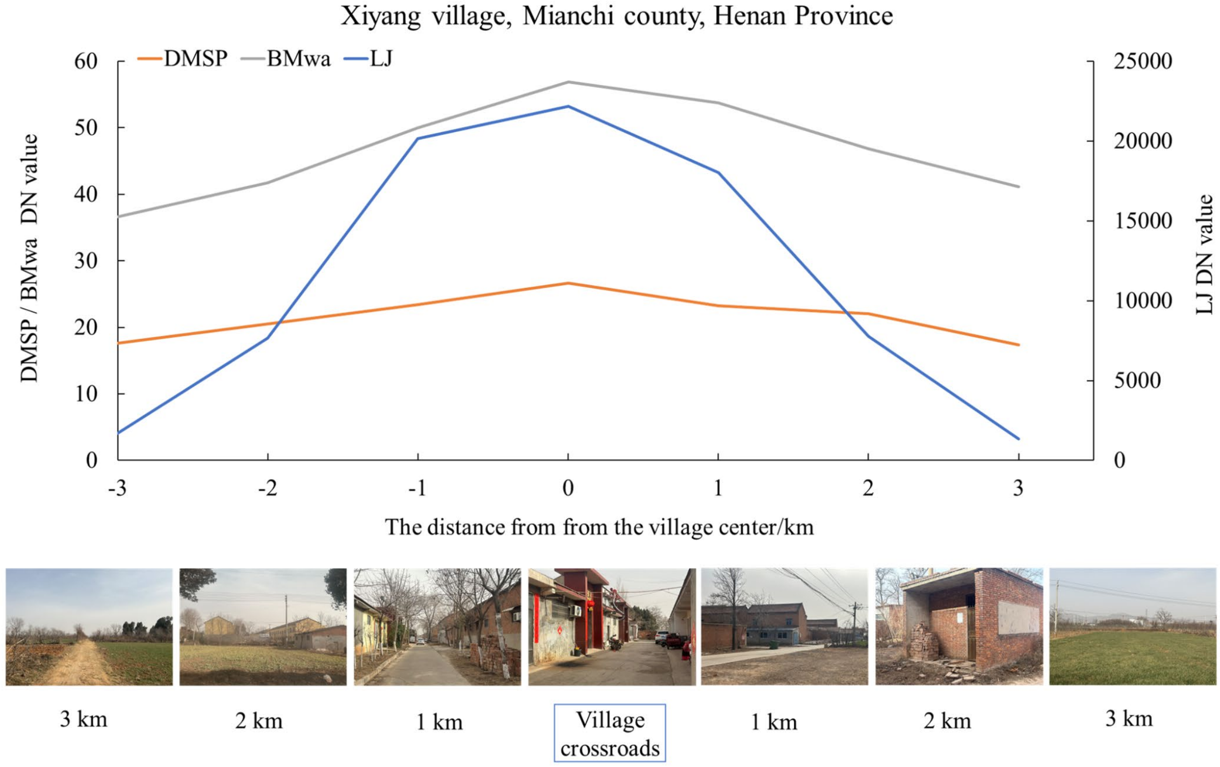


Figure 2: Example of a ground-truthing transect: Xiyang village, Mianchi county, Henan Province

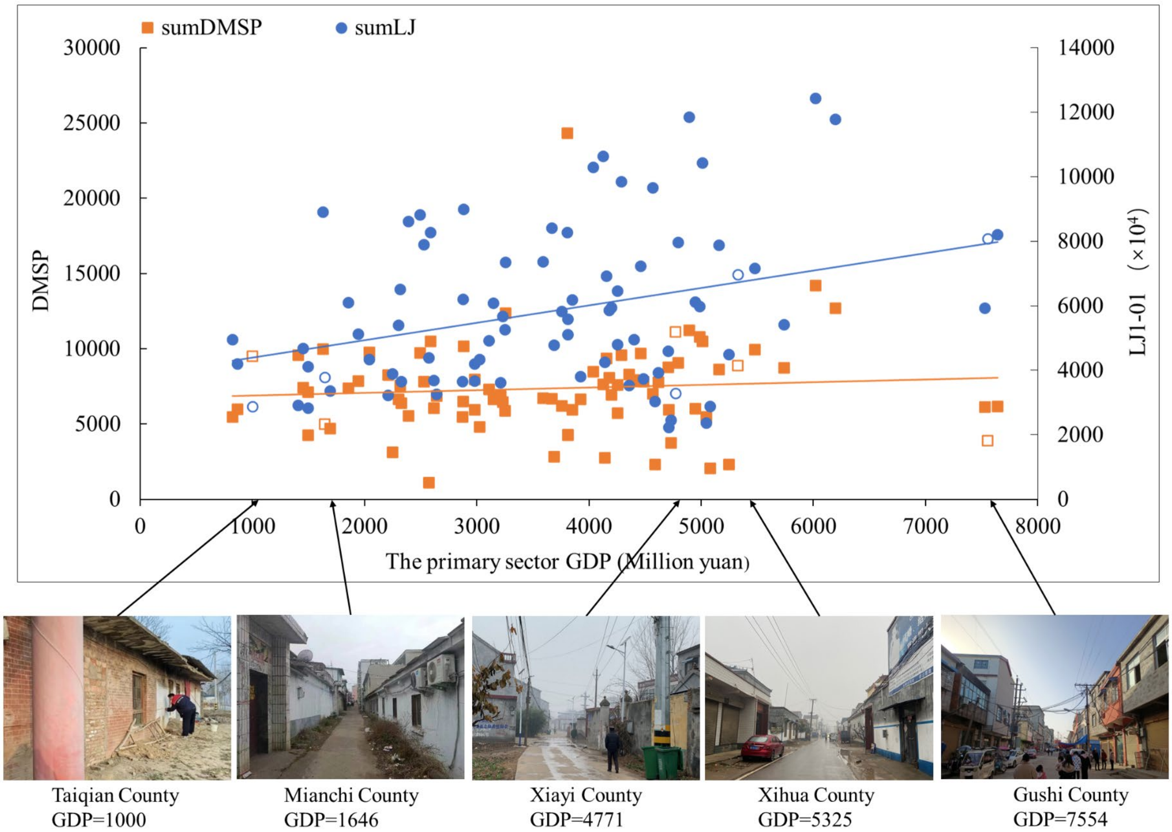


Figure 3: Example of a Primary sector GDP—luminosity curve: Henan Province (hollow symbols are counties where the ground-truthing photographs are taken)

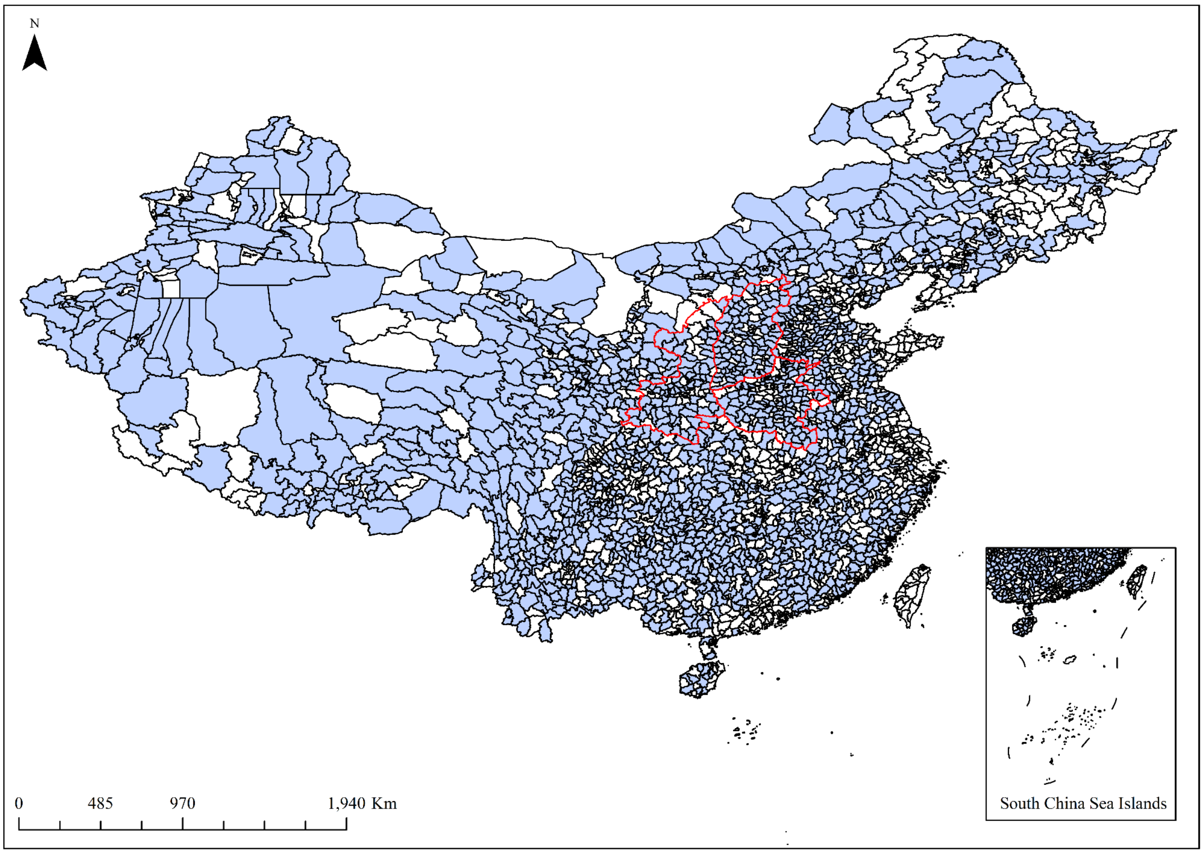


Figure 4: Location map for the $n$=1460 rural counties
(provinces with red borders had ground-truthing exercises)

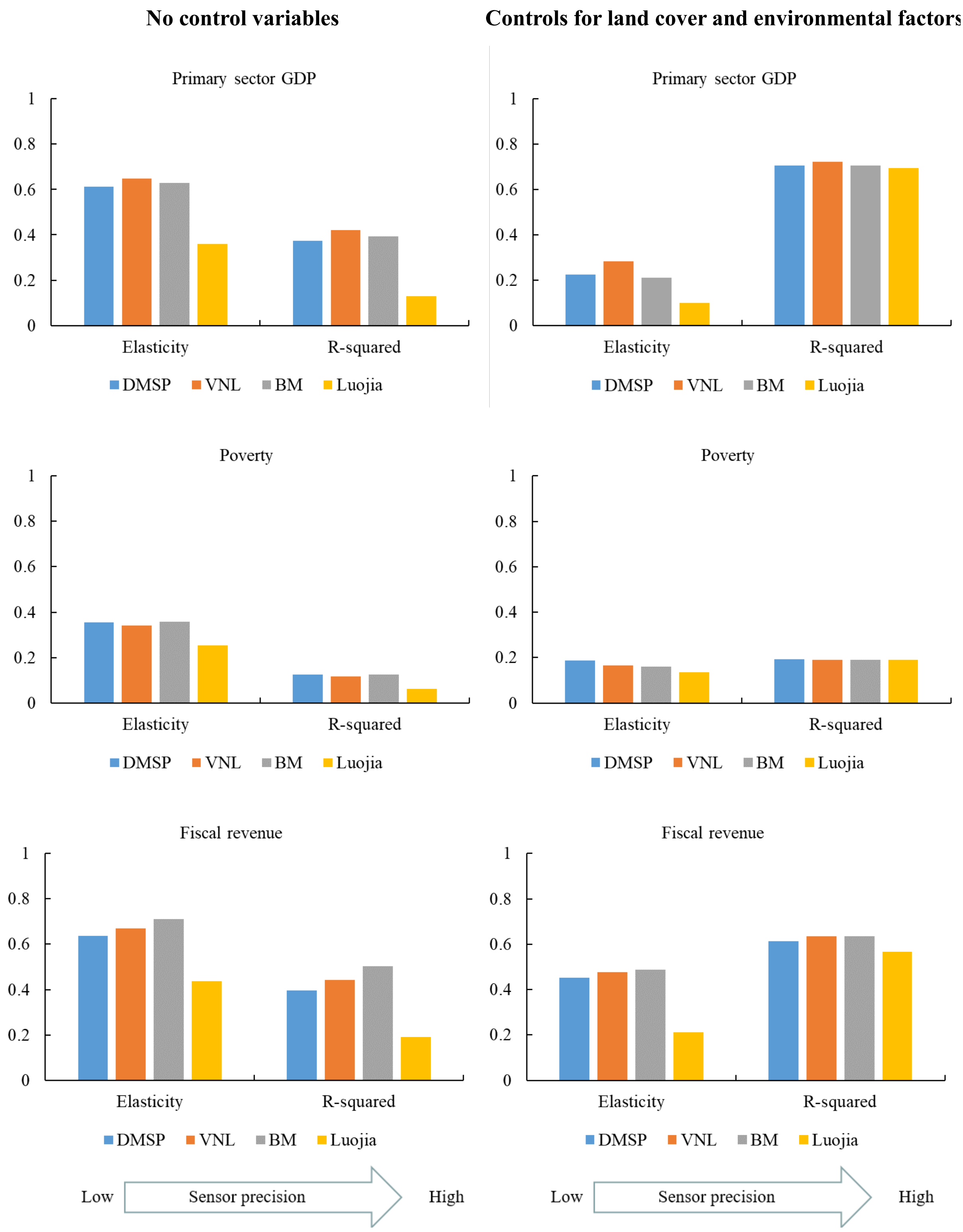


Figure 5: Variation in the Predictive Performance of NTL data from Sensors of Varying Precision
*Notes:* Based on *n*=1460 counties, with full results reported in Tables 1-3 of Appendix C. The sign of the elasticities of poverty with respect to luminosity are reversed for display purposes. The luminosity indicator used is the sum of lights. The R-squared reported is the adjusted R-squared to account for the different number of covariates.

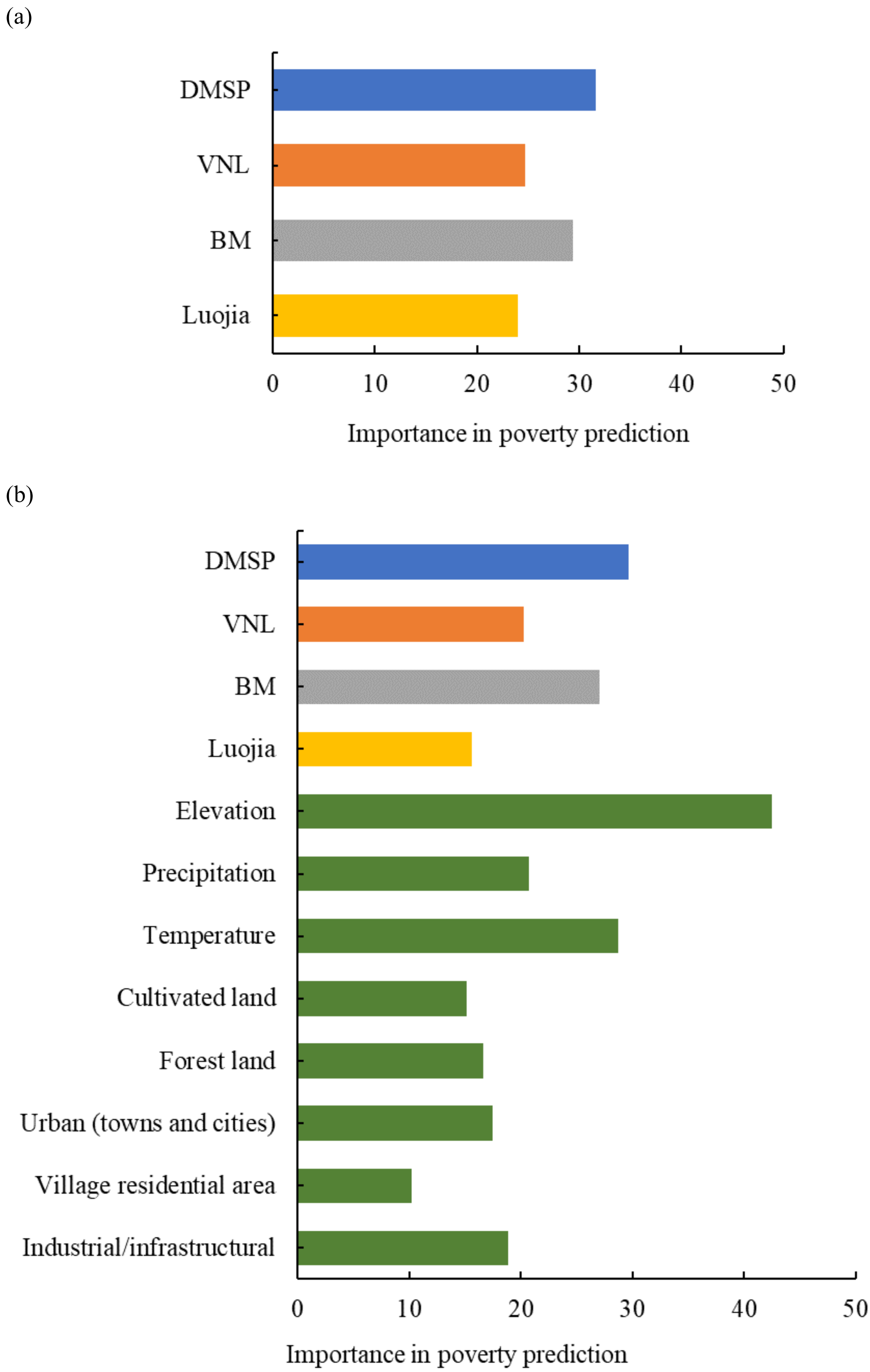


Figure 6. Average contributions of each NTL variable to poverty predictions.
*Notes*: (a) only includes NTL variables, (b) also includes environmental variables.

# Appendix A: Details on the Ground-Truthing Exercises

We selected sites in three provinces (Henan, Shanxi, and Shaanxi) for ground-truthing exercises that aimed to provide first-hand insight into the ability of Luojia, BM, VNL and DMSP to detect small-scale rural development. We chose these three provinces because of their advantages of adjacency and centrality (for the last several decades both the population-weighted and the GDP-weighted center of China have been located in Henan). As a check on whether these provinces had significant deviations from China's 'typical' relationships between rural economic activity and luminosity we first estimated province-by-province elasticities of primary sector GDP with respect to luminosity (using double-log specifications). The results are in Table 1. For Luojia-01, which is our main sensor of interest, there was no difference between the GDP-luminosity elasticities for these three provinces and for the other provinces (a mean difference of -0.08, $p$<0.54). Likewise, the $R^2$ of the prediction equations was not significantly lower for these three provinces ($p$<0.34). Hence, we expect that our ground-truthing exercises should be broadly informative.

Within these three provinces, we chose ground-truthing sites that took into account varying wealth levels and varying levels of economic activity, while also achieving a spatial spread of locations in each province (Figures 1a, 2a, and 3a shows these locations). We took a field trip to each location, and selected villages for more detailed study by taking transects from the village centers. We then plot radiance along the same transect. For example, in Figures 1c, 2c, and 3c it can be seen that Luojia-01 radiance is very low/zero outside the village and then spikes in the village center and goes back to being very low. In contrast, DMSP tends to not show much variation along the transect, most likely because of blurring problems. Even though the resolution of the Black Marble and VNL data is much better than for DMSP, these sources also tended to obscure the differences seen on the ground along the village transects. In other words, at a very fine scale the Luojia data seem to have more sensitivity to reflect economic activities in China's rural areas that are less well detected by the other sensors.

Moving from the village to the county level, we plotted primary sector GDP against luminosity and illustrated at various points the difference in on-the-ground conditions (Figures 1b, 2b, 3b). For example, in Henan province there is no relationship between luminosity and county primary sector GDP when using DMSP data, while the Luojia data are positively correlated with GDP (and more closely related to GDP than are VNL or BM data). The scatter plots for the other two provinces do not show such marked contrasts between the various remote sensing data sources.

Table 1: Province-by-province elasticities of primary sector GDP with respect to luminosity

| | DMSP | VNL | Black Marble | Luojia-01 |
|---|---|---|---|---|
| *Ground-truthing provinces* | | | | |
| Shanxi | 0.463*** | 0.364** | 0.396*** | 0.275* |
| | (0.115) | (0.122) | (0.099) | (0.118) |
| Henan | 0.039 | 0.174 | 0.122 | 0.283** |
| | (0.115) | (0.113) | (0.091) | (0.109) |
| Shaanxi | 0.325*** | 0.433*** | 0.314*** | 0.339*** |
| | (0.072) | (0.087) | (0.069) | (0.099) |
| *Other provinces* | | | | |
| Hebei | 0.343*** | 0.320** | 0.297*** | 0.233** |
| | (0.098) | (0.104) | (0.088) | (0.072) |
| Inner Mongolia | 0.505*** | 0.627*** | 0.474*** | 0.251* |
| | (0.106) | (0.108) | (0.097) | (0.130) |
| Liaoning | -0.016 | 0.179 | 0.109 | 0.185 |
| | (0.104) | (0.120) | (0.107) | (0.166) |
| Jilin | 0.815** | 1.114*** | 0.812** | 0.575* |
| | (0.287) | (0.268) | (0.262) | (0.228) |
| Heilongjiang | 0.565*** | 0.620*** | 0.467*** | 0.026 |
| | (0.094) | (0.106) | (0.090) | (0.178) |
| Jiangsu | 0.439* | 0.515*** | 0.391* | 0.463* |
| | (0.177) | (0.127) | (0.156) | (0.175) |
| Zhejiang | 0.432*** | 0.329* | 0.551*** | 0.445* |
| | (0.102) | (0.165) | (0.104) | (0.190) |
| Anhui | 0.468*** | 0.557*** | 0.502*** | 0.697*** |
| | (0.045) | (0.058) | (0.051) | (0.124) |
| Fujian | 0.379*** | 0.533*** | 0.354*** | 0.421*** |
| | (0.087) | (0.106) | (0.083) | (0.116) |
| Jiangxi | 0.540*** | 0.562*** | 0.487*** | 0.586*** |
| | (0.071) | (0.092) | (0.078) | (0.086) |
| Shandong | 0.094 | 0.272* | 0.304** | 0.278* |
| | (0.128) | (0.116) | (0.110) | (0.135) |
| Hubei | 0.494*** | 0.450*** | 0.389** | 0.502*** |
| | (0.099) | (0.127) | (0.128) | (0.103) |
| Hunan | 0.697*** | 0.794*** | 0.596*** | 0.738*** |
| | (0.116) | (0.105) | (0.098) | (0.121) |
| Guangdong | 0.565*** | 0.658*** | 0.547*** | 0.596*** |
| | (0.116) | (0.141) | (0.116) | (0.132) |
| Guangxi | 0.660*** | 0.697*** | 0.714*** | 0.604*** |
| | (0.083) | (0.065) | (0.077) | (0.146) |
| Hainan | 0.713** | 0.658*** | 0.574** | 0.755*** |
| | (0.202) | (0.098) | (0.153) | (0.132) |
| Sichuan | 0.808*** | 0.859*** | 0.839*** | 0.308** |
| | (0.073) | (0.077) | (0.058) | (0.116) |
| Guizhou | 0.531*** | 0.531*** | 0.488*** | 0.146* |
| | (0.106) | (0.096) | (0.111) | (0.077) |
| Yunnan | 0.544*** | 0.535*** | 0.524*** | 0.205** |
| | (0.063) | (0.062) | (0.062) | (0.068) |
| Tibet | 0.083 | 0.549*** | -0.056 | 0.540*** |
| | (0.086) | (0.136) | (0.129) | (0.132) |
| Gansu | 0.270** | 0.513*** | 0.196* | 0.048 |
| | (0.093) | (0.099) | (0.082) | (0.082) |
| Qinghai | 0.361*** | 0.435** | 0.468*** | 0.200 |
| | (0.096) | (0.142) | (0.123) | (0.258) |

| | | | | |
|---|---|---|---|---|
| Ningxia | 0.415* | 0.494* | 0.250 | 0.266* |
| | (0.225) | (0.215) | (0.191) | (0.098) |
| Xinjiang | 0.650*** | 0.726*** | 0.407*** | 0.151 |
| | (0.120) | (0.096) | (0.121) | (0.123) |

*Notes:* Standard errors in ( ), with statistical significance at 1%, 5% or 10% denoted by ***, **, or *.

Figure 1a: Ground-truthing Map for Henan Province.

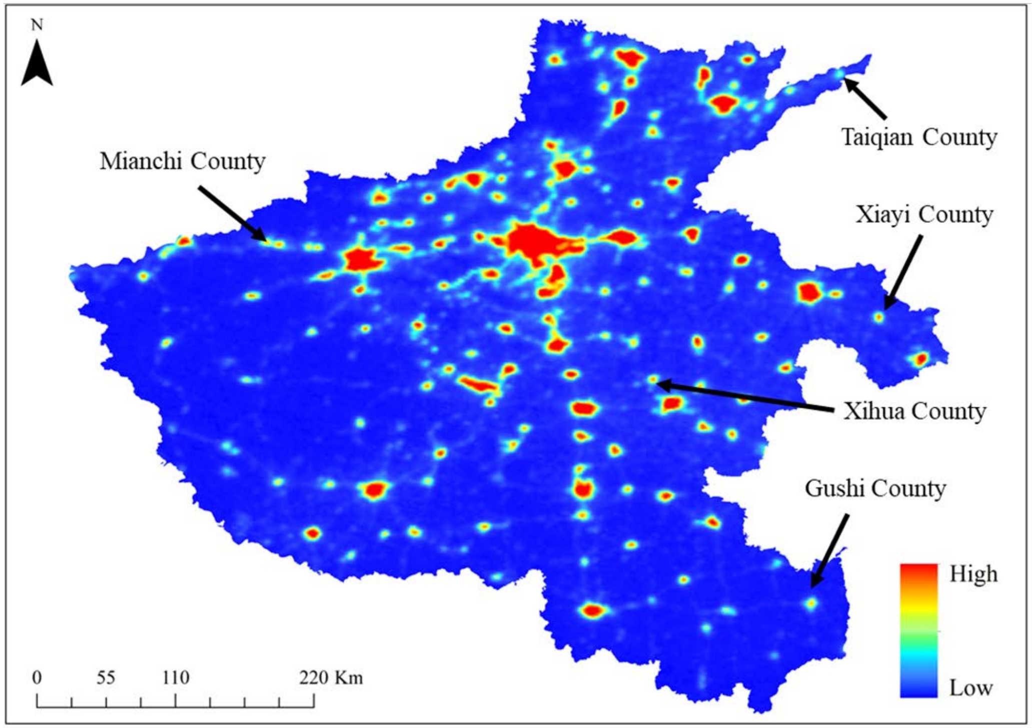


DMSP

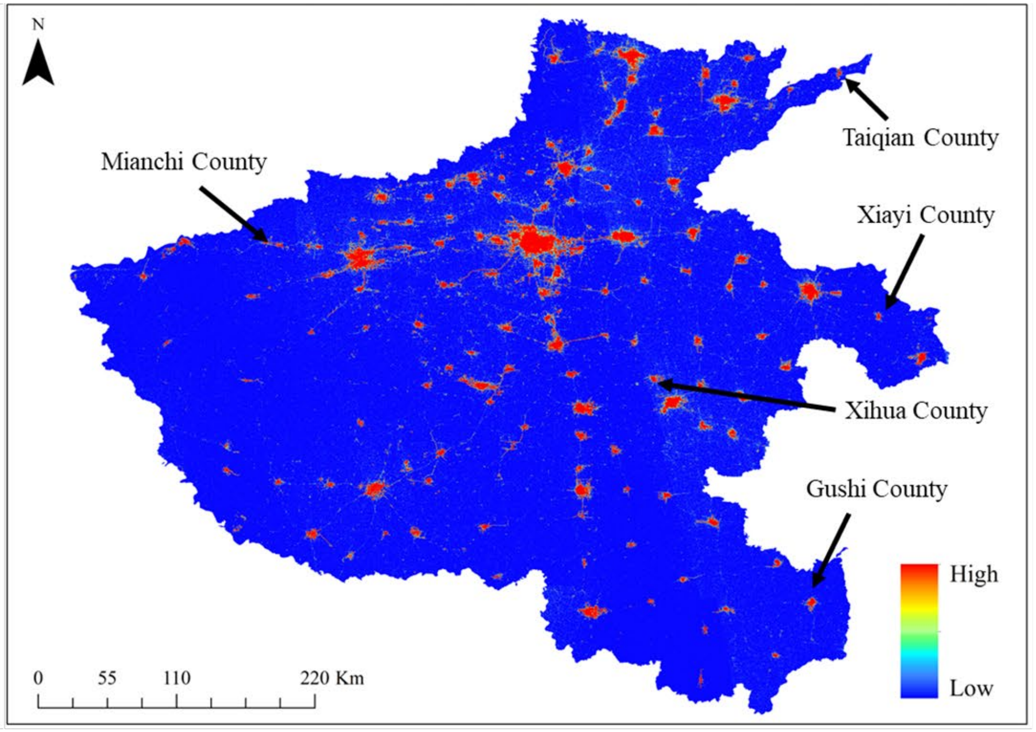


Luojia

Note: The selected counties for ground-truthing are named in the image.

Figure 1b: Scatter plot of Henan Province.

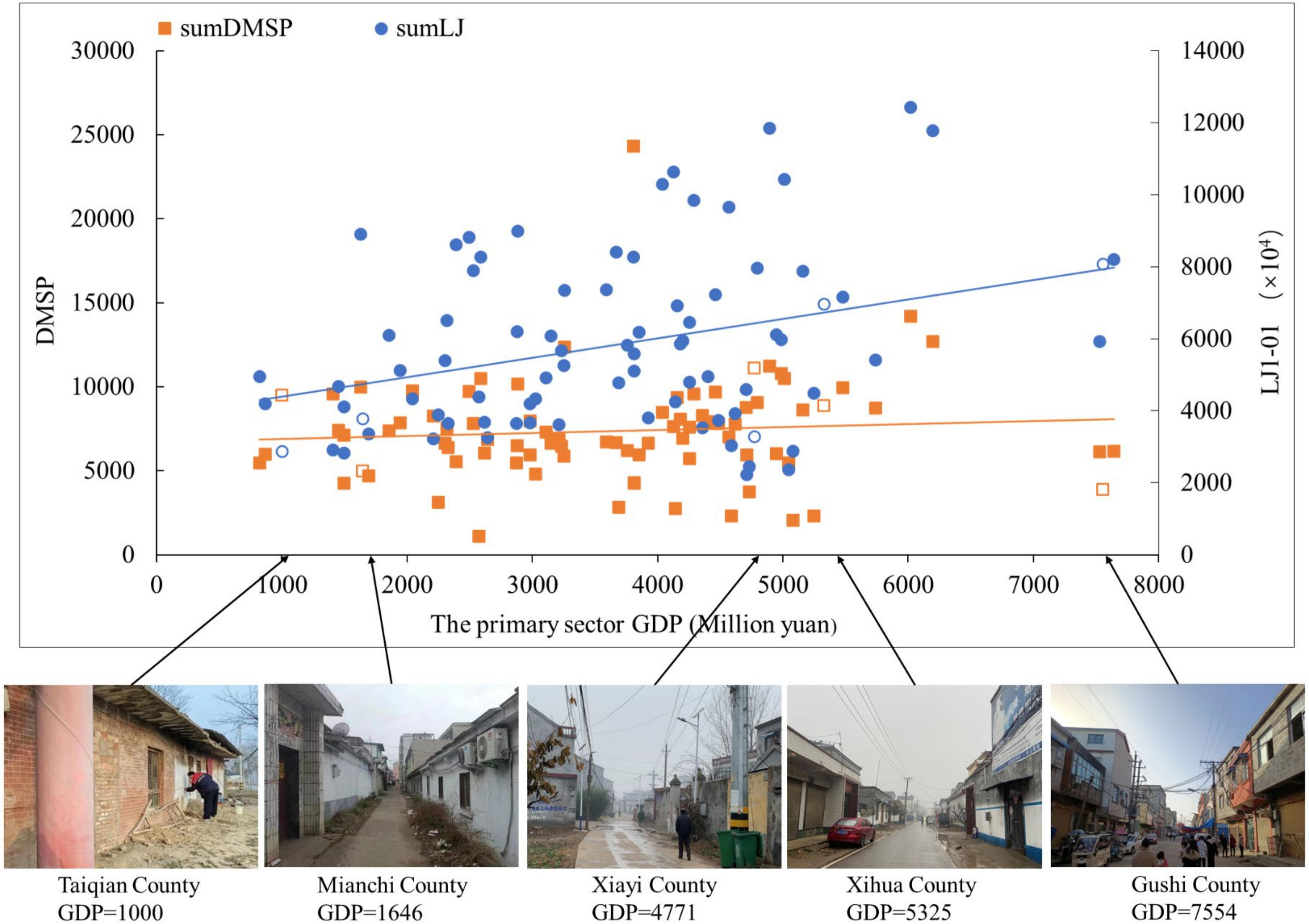

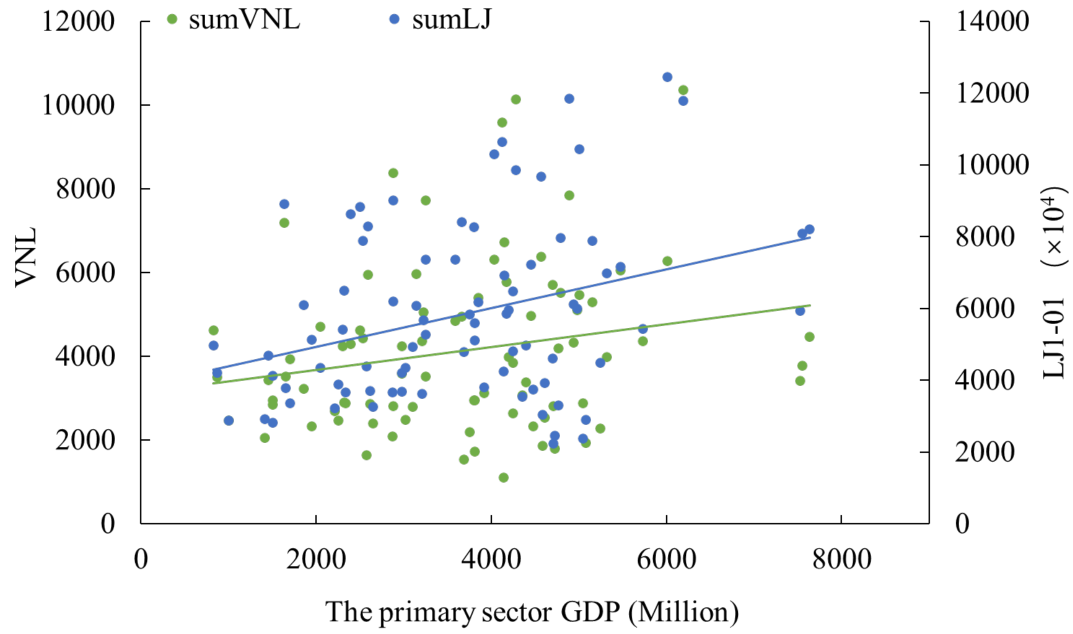

sumVNL
sumLJ
VNL
LJ1-01 （×10⁴）
The primary sector GDP (Million)


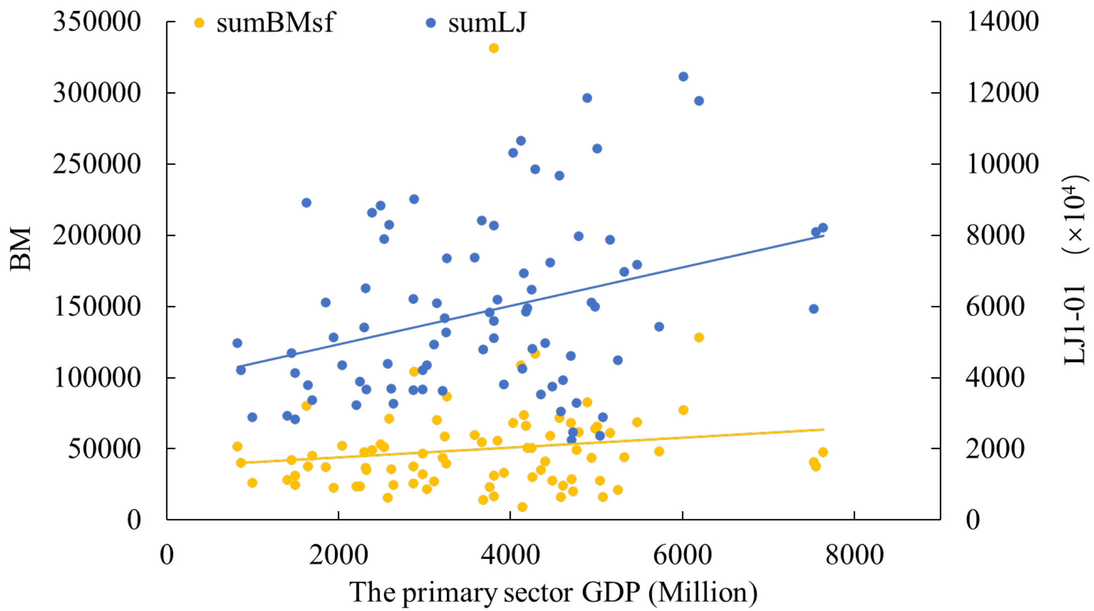

sumBMsf
sumLJ
BM
LJ1-01 （×10⁴）
The primary sector GDP (Million)

Figure 1c: The transects map for Xiyang village, Mianchi county, Henan Province.

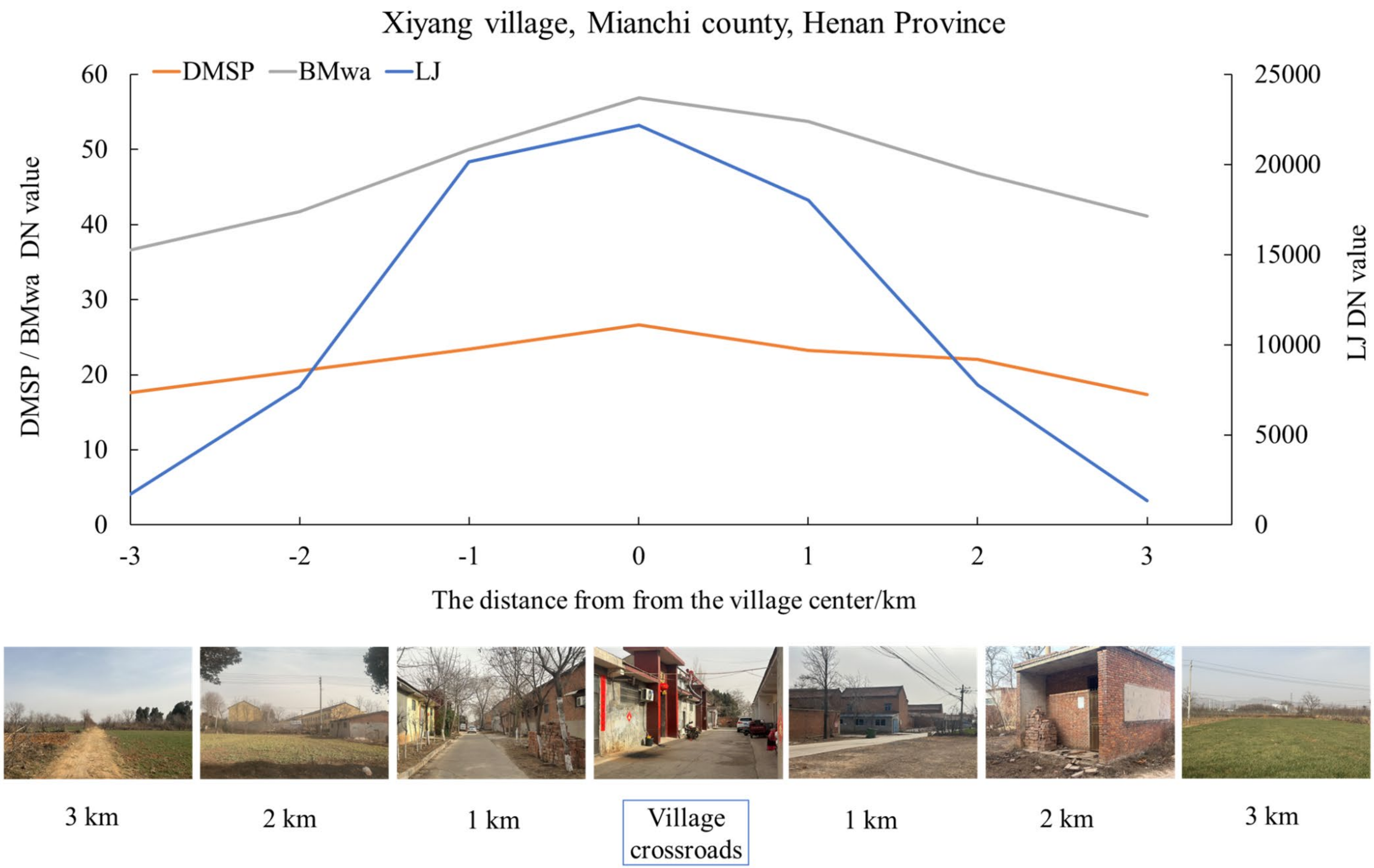

Figure 2a: Ground-truthing Map for Shanxi Province.

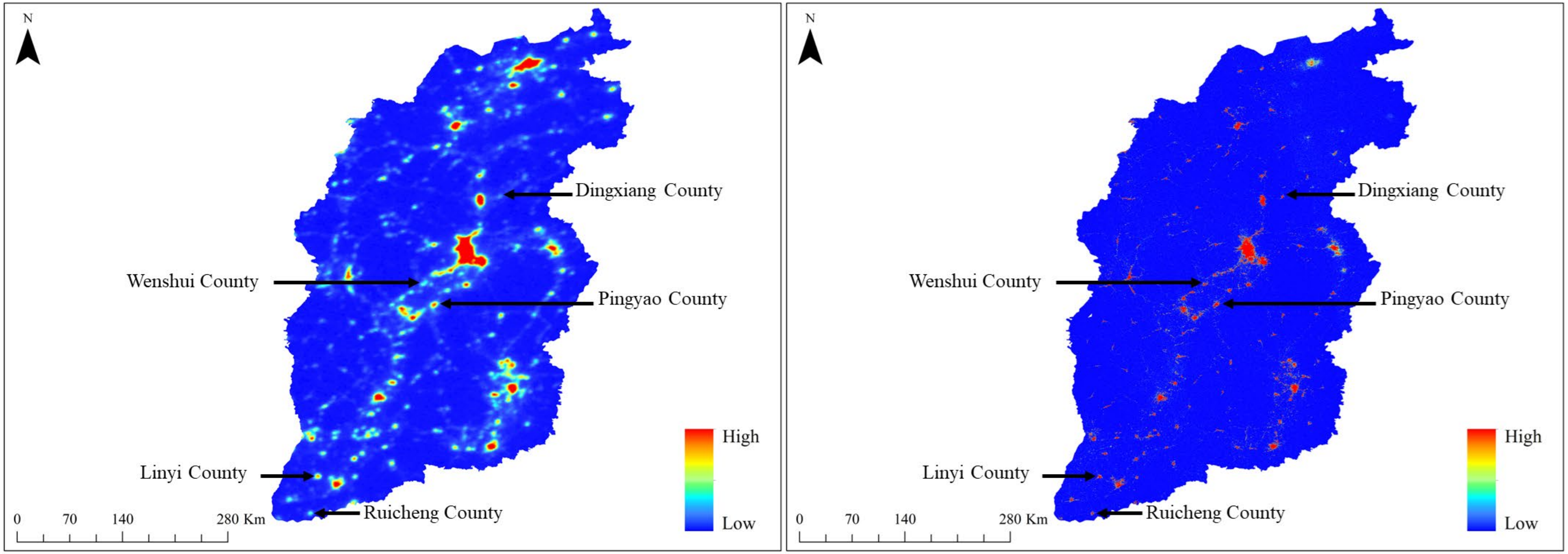


DMSP Luojia

Note: The selected counties for ground-truthing are named in the image.

Figure 2b: Scatter plot of Shanxi Province.

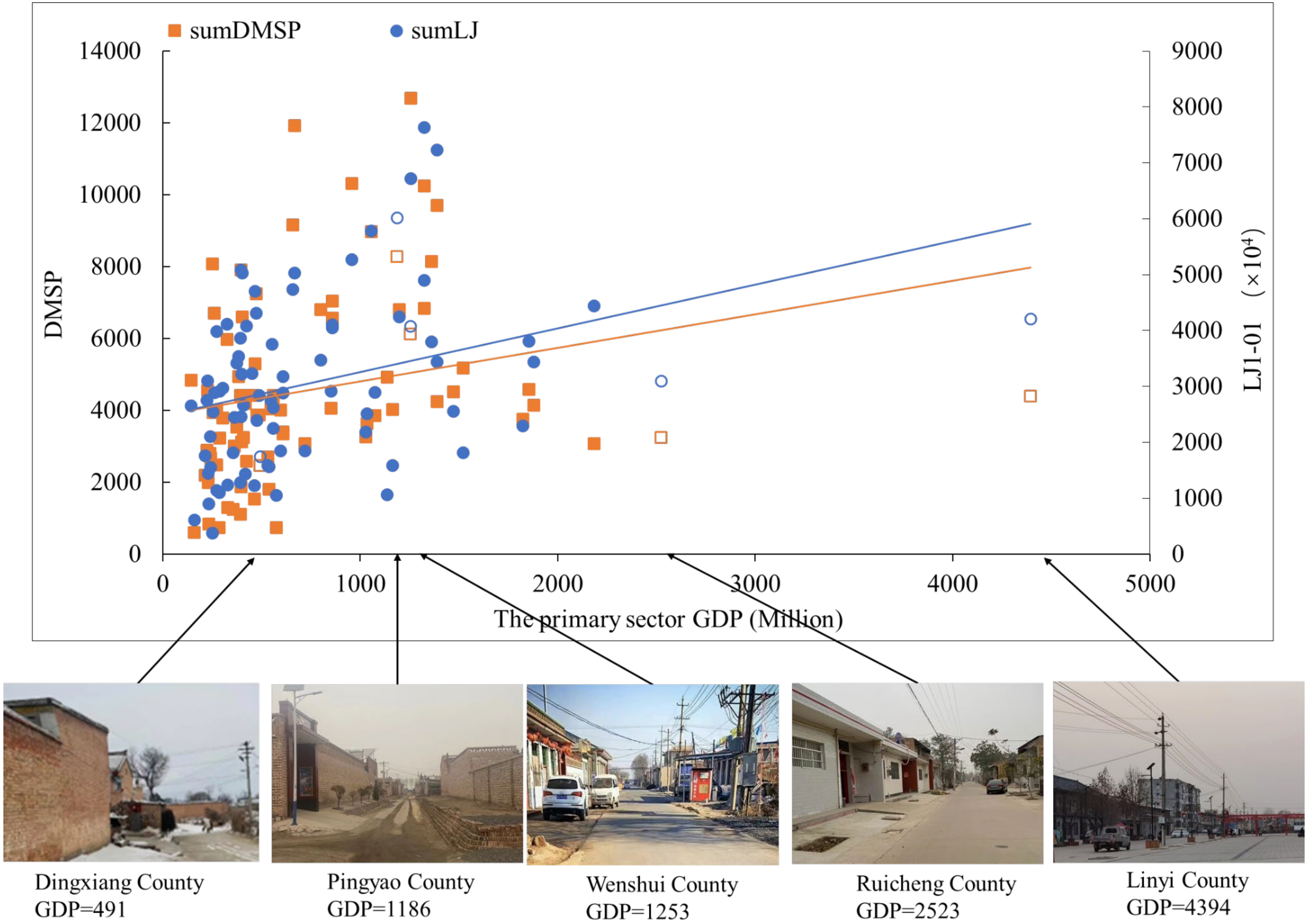

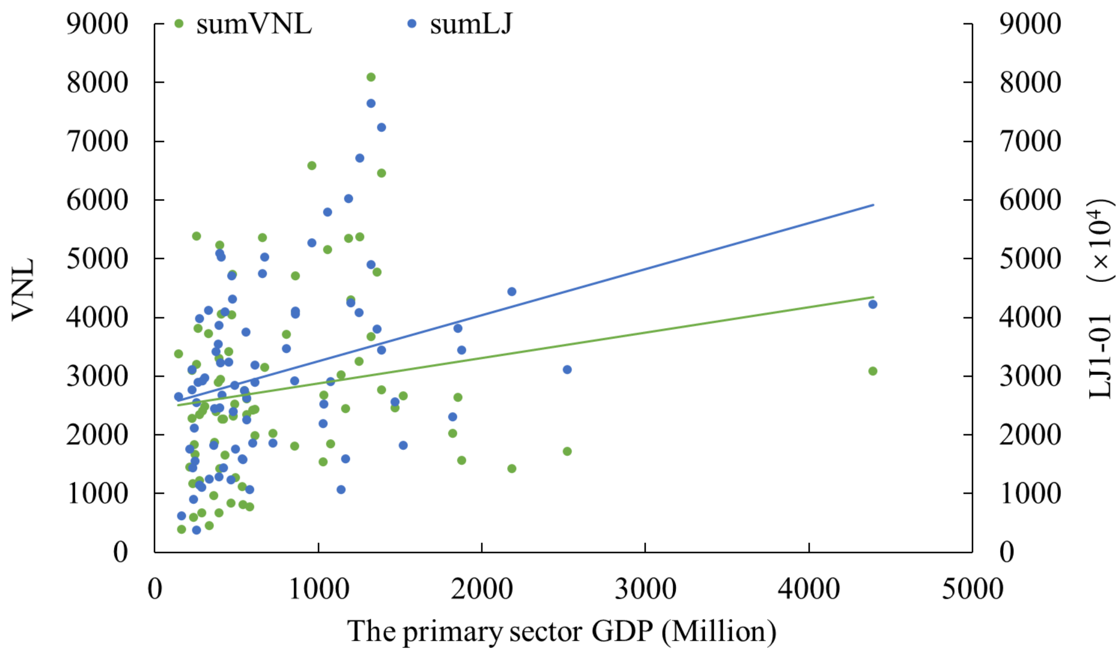

sumVNL
sumLJ
VNL
LJ1-01 (×10⁴)
The primary sector GDP (Million)
0
1000
2000
3000
4000
5000
6000
7000
8000
9000


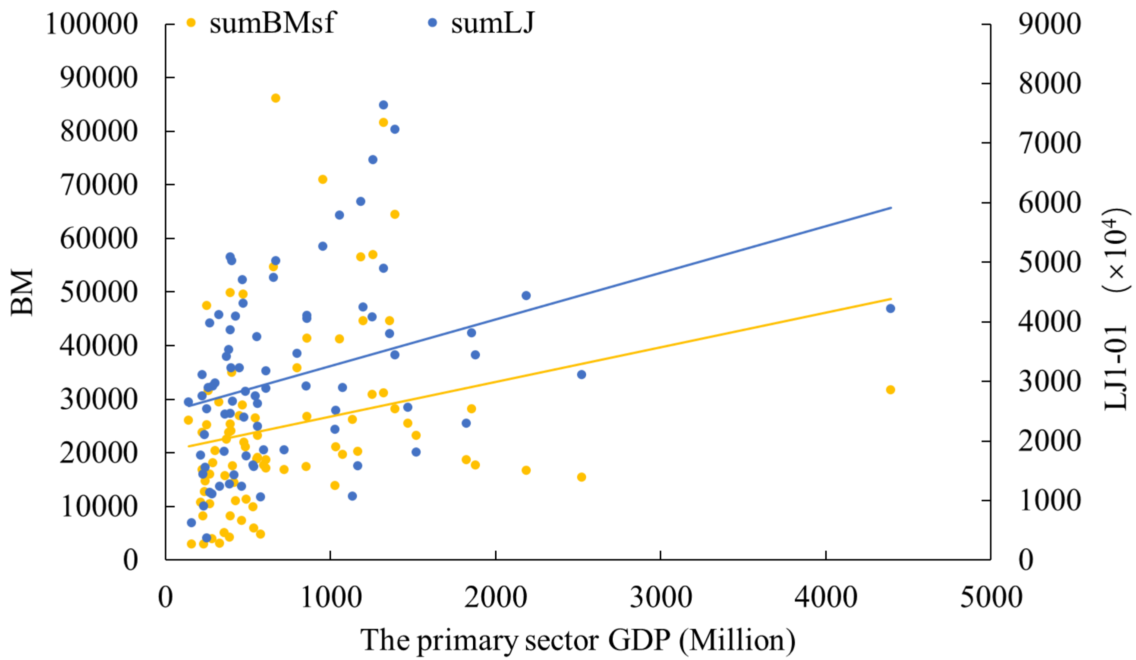

sumBMsf
sumLJ
BM
LJ1-01 (×10⁴)
The primary sector GDP (Million)
0
10000
20000
30000
40000
50000
60000
70000
80000
90000
100000

Figure 2c: The transects map for Dajianbei village, Pinglu county, Shanxi Province.

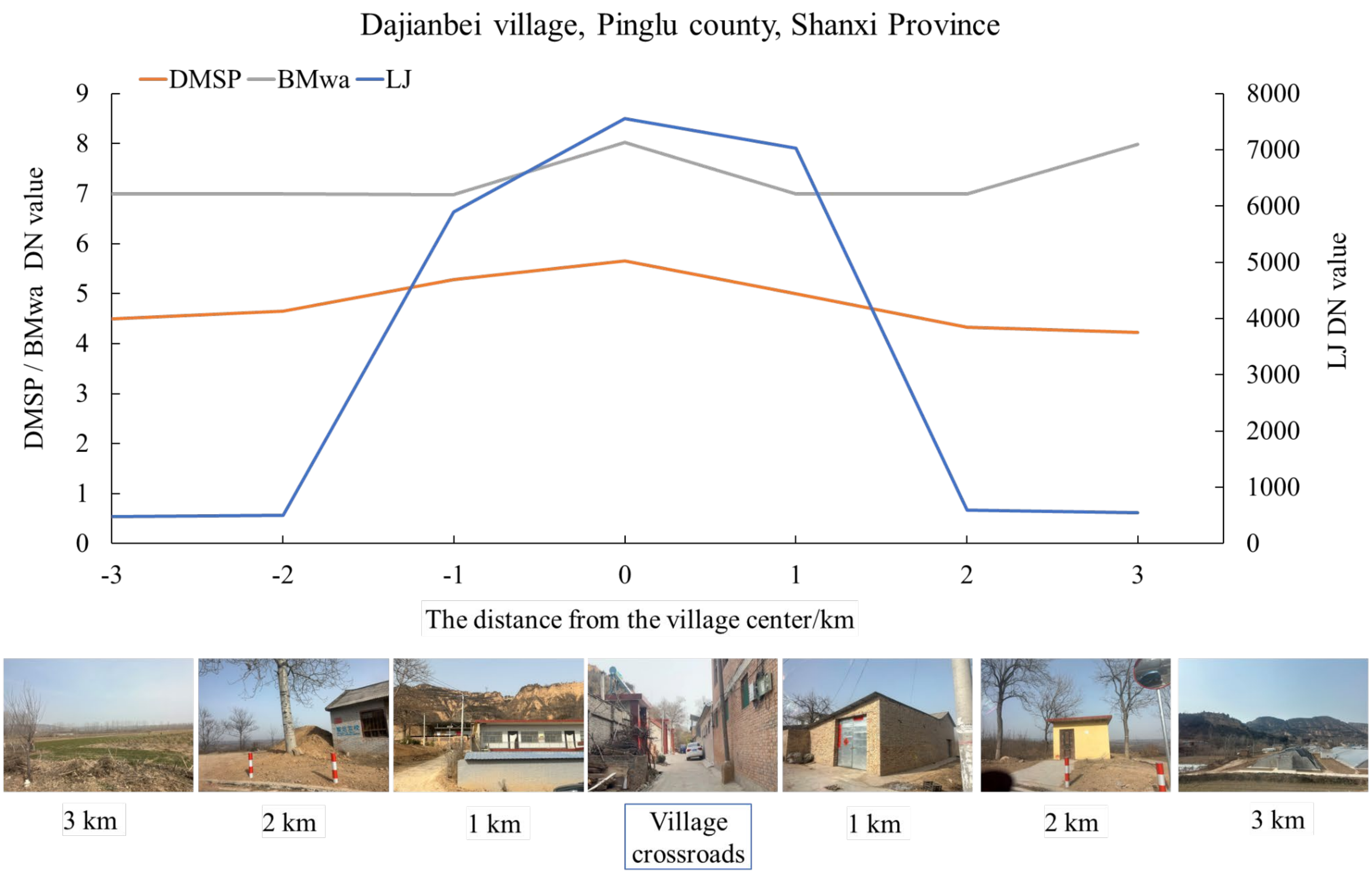

Figure 3a: Ground-truthing Map for Shaanxi Province.

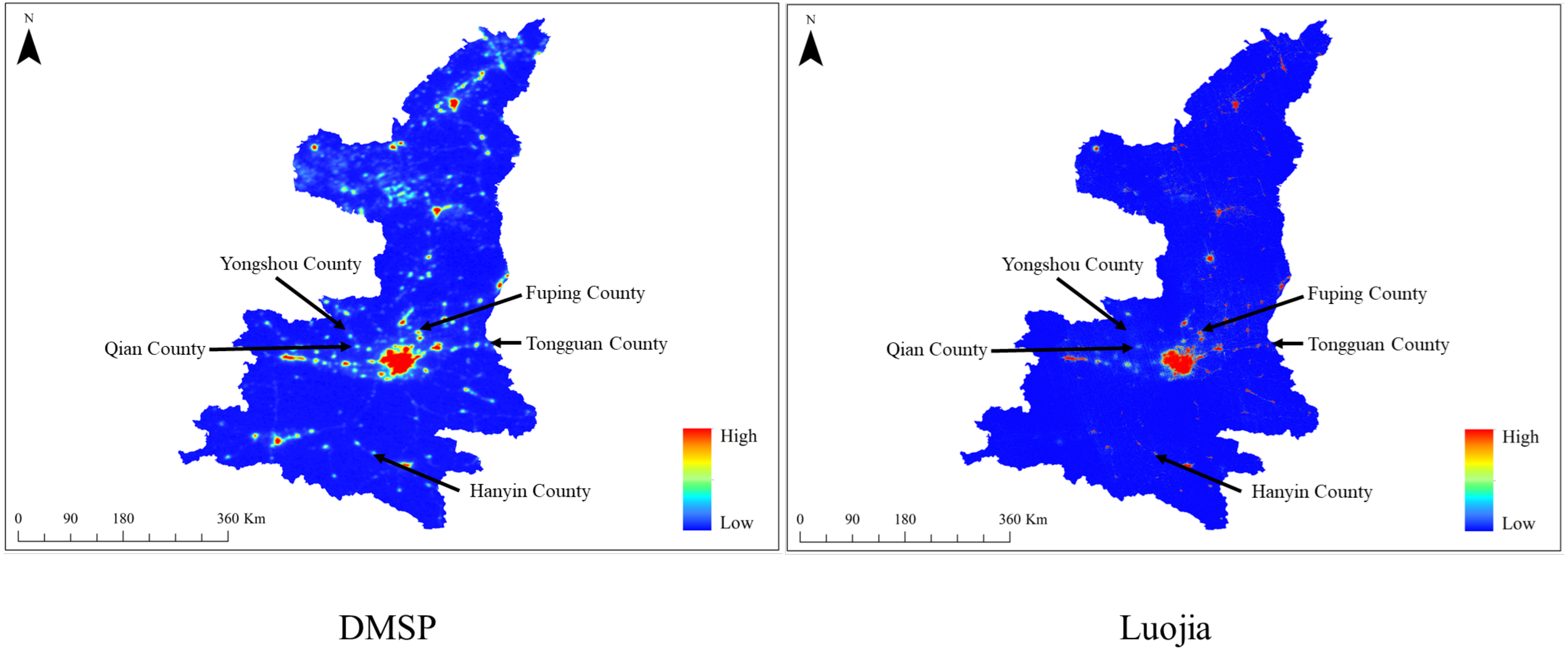


Note: The selected counties for ground-truthing are named in the image.

Figure 3b: Scatter plot of Shaanxi Province.

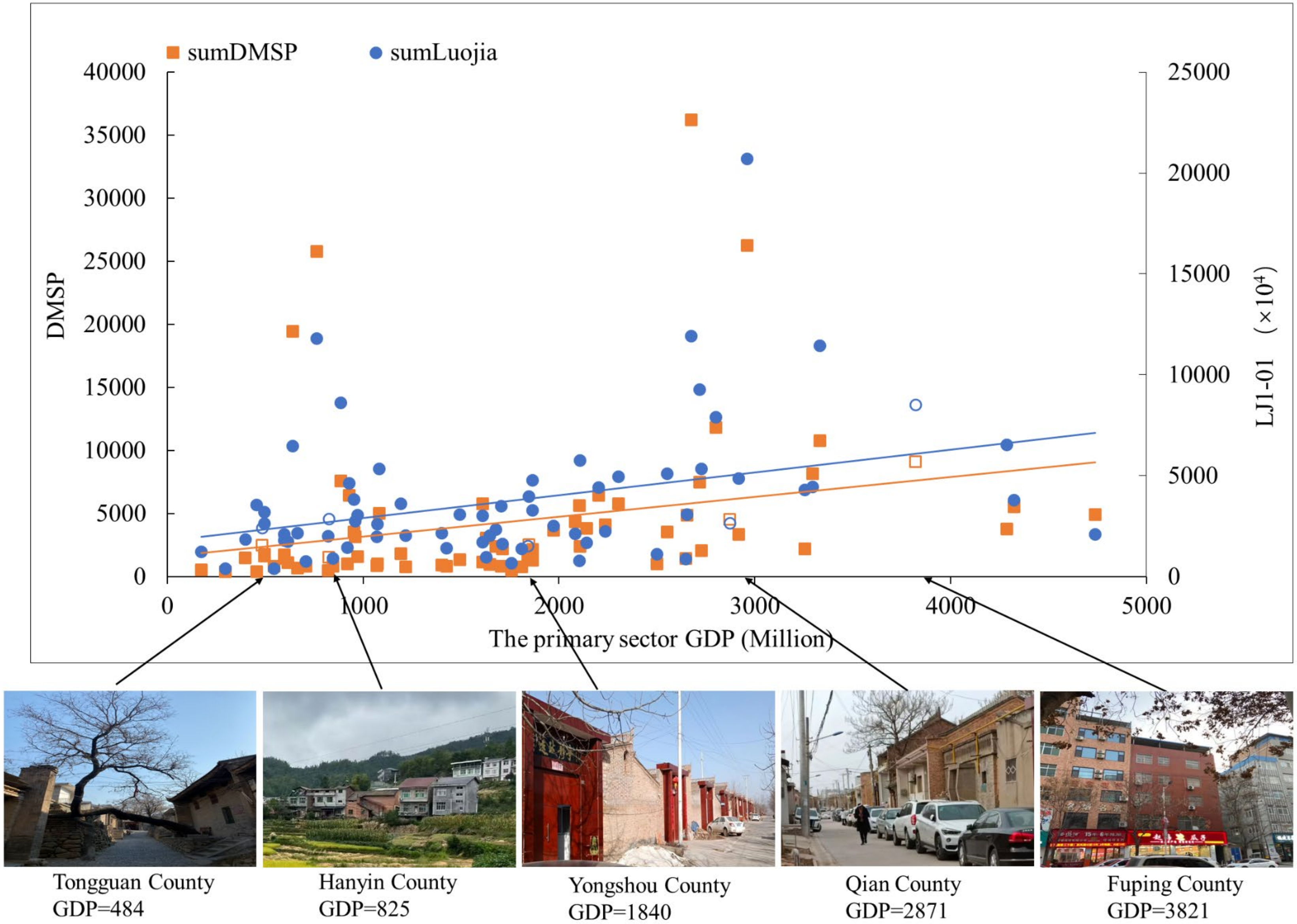

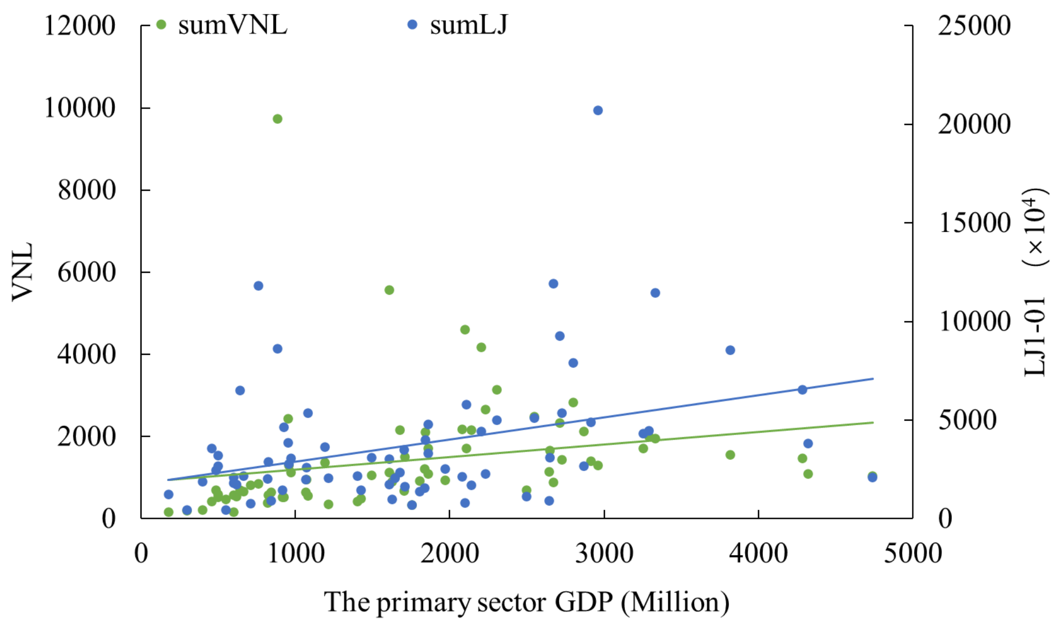
sumVNL
sumLJ
VNL
LJ1-01 (×10^4)
The primary sector GDP (Million)
12000
10000
8000
6000
4000
2000
0
25000
20000
15000
10000
5000
0
1000
2000
3000
4000
5000

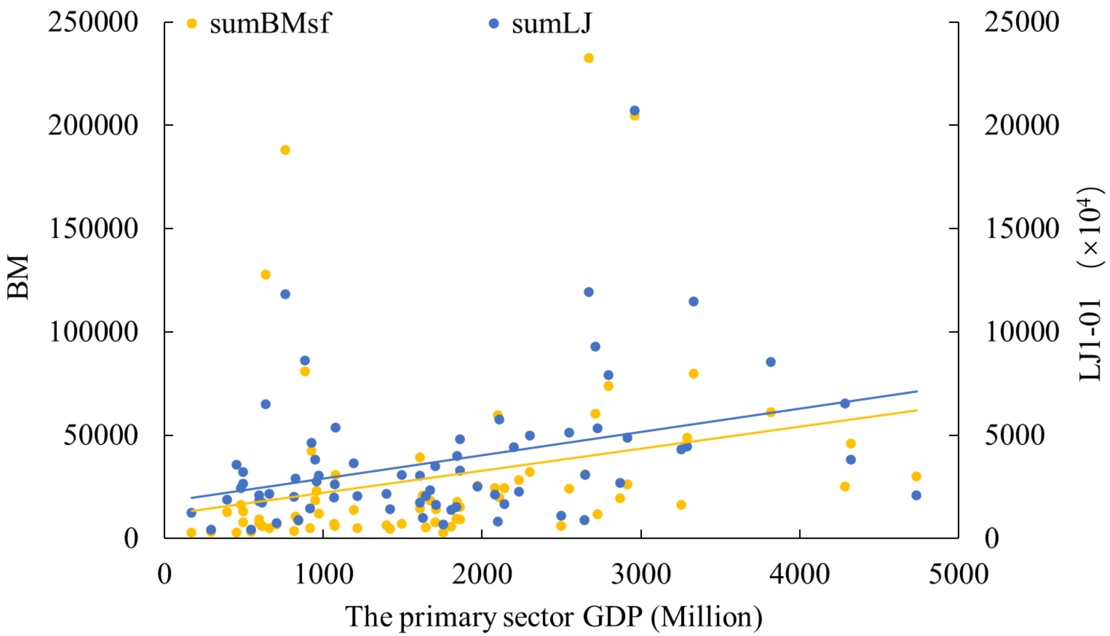
sumBMsf
sumLJ
BM
LJ1-01 (×10^4)
The primary sector GDP (Million)
250000
200000
150000
100000
50000
0
25000
20000
15000
10000
5000
0
1000
2000
3000
4000
5000

Figure 3c: The transects map for Sidi village, Tongguan county, Shaanxi Province.

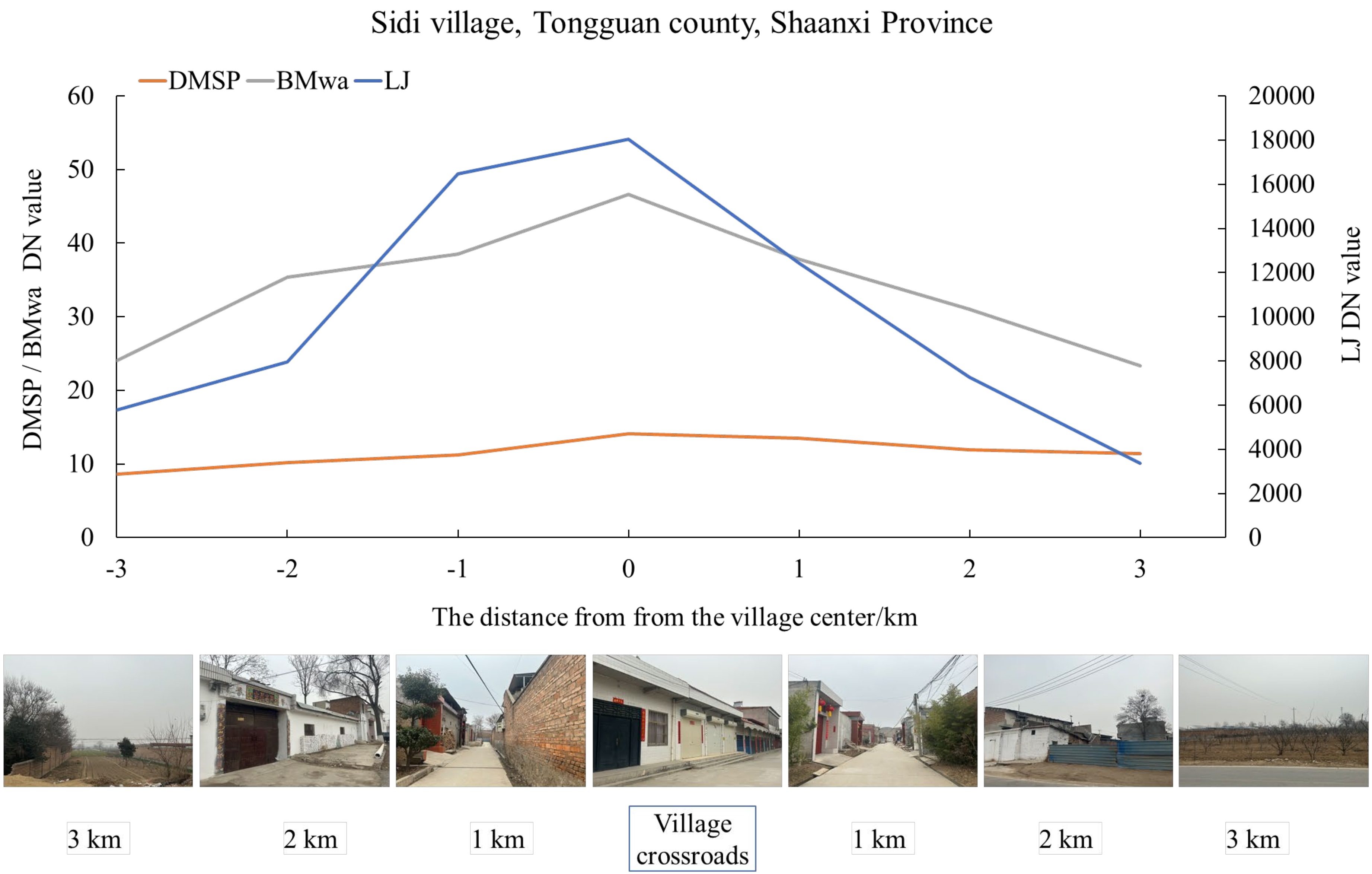

## Appendix B: Sample Selection Flowchart

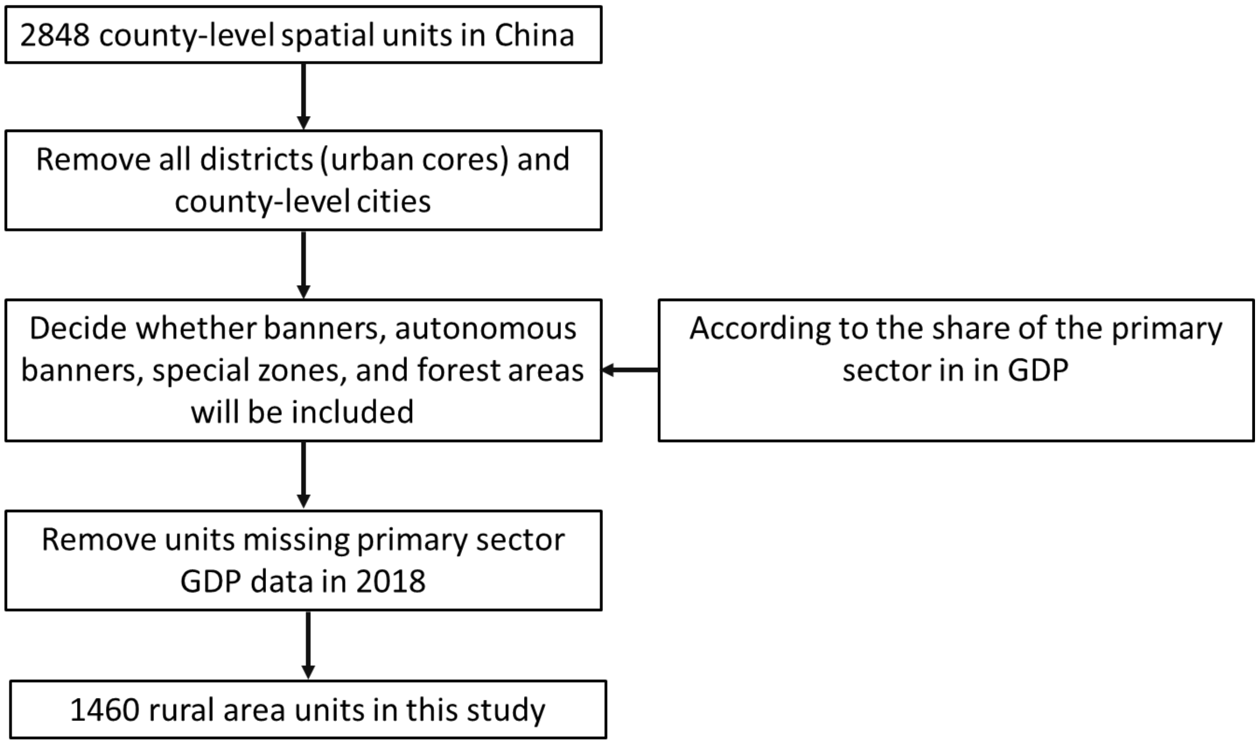

## Appendix C: Detailed Regression Results for Primary Sector GDP, Poverty Status and Fiscal Revenue

Table 1: The predictive power of night-time lights data for primary sector GDP in rural areas of China

| | No control variables | | | Controls for land cover and environmental factors | | |
|---|---|---|---|---|---|---|
| | ln (sum of lights) | ln (lights per km$^2$) | % of pixels illuminated | ln (sum of lights) | ln (lights per km$^2$) | % of pixels illuminated |
| DMSP | 0.612*** | 0.559*** | 0.571*** | 0.226*** | 0.084*** | 0.080*** |
| | (0.021) | (0.022) | (0.022) | (0.023) | (0.024) | (0.025) |
| **Adjusted $R^2$** | **0.374** | **0.313** | **0.325** | **0.705** | **0.688** | **0.688** |
| DMSP F15 | 0.597*** | 0.552*** | 0.567*** | 0.197*** | 0.076*** | 0.083*** |
| | (0.021) | (0.022) | (0.022) | (0.022) | (0.024) | (0.025) |
| **Adjusted $R^2$** | **0.357** | **0.304** | **0.322** | **0.702** | **0.688** | **0.688** |
| DMSP F16 | 0.606*** | 0.559*** | 0.563*** | 0.234*** | 0.091*** | 0.074*** |
| | (0.021) | (0.022) | (0.022) | (0.023) | (0.024) | (0.025) |
| **Adjusted $R^2$** | **0.366** | **0.312** | **0.316** | **0.707** | **0.689** | **0.687** |
| VIIRS Night Lights | 0.648*** | 0.569*** | 0.527*** | 0.283*** | 0.122*** | 0.036 |
| | (0.020) | (0.022) | (0.022) | (0.021) | (0.024) | (0.025) |
| **Adjusted $R^2$** | **0.420** | **0.323** | **0.277** | **0.721** | **0.691** | **0.686** |
| Black Marble, weighted average | 0.628*** | 0.560*** | 0.410*** | 0.210*** | 0.083*** | 0.011 |
| | (0.020) | (0.022) | (0.024) | (0.022) | (0.025) | (0.023) |
| **Adjusted $R^2$** | **0.394** | **0.314** | **0.168** | **0.704** | **0.688** | **0.685** |
| Black Marble, snow-free | 0.621*** | 0.557*** | 0.551*** | 0.199*** | 0.081*** | 0.061** |
| | (0.021) | (0.022) | (0.022) | (0.022) | (0.025) | (0.026) |
| **Adjusted $R^2$** | **0.385** | **0.310** | **0.303** | **0.703** | **0.688** | **0.687** |
| Luojia-01 | 0.359*** | 0.440*** | 0.279*** | 0.107*** | 0.028*** | 0.031* |
| | (0.024) | (0.024) | (0.025) | (0.017) | (0.020) | (0.017) |
| **Adjusted $R^2$** | **0.128** | **0.193** | **0.077** | **0.694** | **0.686** | **0.686** |

*Notes:* The dependent variable is the logarithm of primary sector GDP. Coefficients are for standardized variables to aid comparability across outcomes and specifications of NTL data. The sample is $n$=1460 rural counties. Robust standard errors in ( ), $^{***}$, $^{**}$, and $^{*}$ denote statistical significance at 1%, 5% and 10% levels. The control variables in columns (4) to (6) are elevation, precipitation, temperature, and five types of land cover (urban, village, industrial and infrastructural, cultivated land and forest ).

Table 2: The predictive power of night-time lights data for poverty status in rural areas of China

| | No control variables | | | Controls for land cover and environmental factors | | |
|---|---|---|---|---|---|---|
| | ln (sum of lights) | ln (lights per km$^2$) | % of pixels illuminated | ln (sum of lights) | ln (lights per km$^2$) | % of pixels illuminated |
| DMSP | -0.355*** | -0.371*** | -0.356*** | -0.186*** | -0.169*** | -0.146*** |
| | (0.024) | (0.024) | (0.024) | (0.038) | (0.039) | (0.040) |
| **Adjusted $R^2$** | **0.126** | **0.137** | **0.126** | **0.192** | **0.189** | **0.185** |
| DMSP F15 | -0.351*** | -0.369*** | -0.361*** | -0.176*** | -0.168*** | -0.158*** |
| | (0.025) | (0.024) | (0.024) | (0.036) | (0.038) | (0.040) |
| **Adjusted $R^2$** | **0.123** | **0.136** | **0.130** | **0.191** | **0.189** | **0.187** |
| DMSP F16 | -0.347*** | -0.367*** | -0.349*** | -0.175*** | -0.160*** | -0.116*** |
| | (0.025) | (0.024) | (0.025) | (0.038) | (0.039) | (0.040) |
| **Adjusted $R^2$** | **0.120** | **0.134** | **0.121** | **0.190** | **0.188** | **0.183** |
| VIIRS Night Lights | -0.342*** | -0.360*** | -0.345*** | -0.165*** | -0.158*** | -0.111*** |
| | (0.025) | (0.024) | (0.025) | (0.036) | (0.038) | (0.040) |
| **Adjusted $R^2$** | **0.117** | **0.129** | **0.119** | **0.190** | **0.187** | **0.182** |
| Black Marble, weighted average | -0.357*** | -0.367*** | -0.343*** | -0.159*** | -0.164*** | -0.146*** |
| | (0.024) | (0.024) | (0.025) | (0.036) | (0.040) | (0.036) |
| **Adjusted $R^2$** | **0.127** | **0.134** | **0.117** | **0.189** | **0.188** | **0.187** |
| Black Marble, snow-free | -0.349*** | -0.362*** | -0.250*** | -0.142*** | -0.153*** | -0.113*** |
| | (0.025) | (0.024) | (0.025) | (0.036) | (0.040) | (0.042) |
| **Adjusted $R^2$** | **0.121** | **0.131** | **0.122** | **0.187** | **0.186** | **0.182** |
| Luojia-01 | -0.255*** | -0.346*** | -0.205*** | -0.136*** | -0.155*** | -0.143*** |
| | (0.025) | (0.025) | (0.025) | (0.028) | (0.032) | (0.028) |
| **Adjusted $R^2$** | **0.064** | **0.120** | **0.093** | **0.191** | **0.191** | **0.193** |

*Notes:* The dependent variable indicates the poverty status of each county. Coefficients are for standardized variables to aid comparability across outcomes and specifications of NTL data. The sample is $n$=1460 rural counties. Robust standard errors in ( ), $^{***}$, $^{**}$, and $^{*}$ denote statistical significance at 1%, 5% and 10% levels. The control variables in columns (4) to (6) are elevation, precipitation, temperature, and five types of land cover (urban, village, industrial and infrastructural, cultivated land and forest ).

Table 3: The predictive power of night-time lights data for county fiscal revenue in rural areas of China

| | No control variables | | | Controls for land cover and environmental factors | | |
|---|---|---|---|---|---|---|
| | ln (sum of lights) | ln (lights per km$^2$) | % of pixels illuminated | ln (sum of lights) | ln (lights per km$^2$) | % of pixels illuminated |
| DMSP | 0.636*** | 0.618*** | 0.606*** | 0.451*** | 0.338*** | 0.313*** |
| | (0.021) | (0.021) | (0.021) | (0.026) | (0.028) | (0.029) |
| **Adjusted $R^2$** | **0.397** | **0.378** | **0.361** | **0.614** | **0.580** | **0.569** |
| DMSP F15 | 0.630*** | 0.616*** | 0.609*** | 0.412*** | 0.328*** | 0.323*** |
| | (0.021) | (0.021) | (0.021) | (0.025) | (0.028) | (0.029) |
| **Adjusted $R^2$** | **0.390** | **0.375** | **0.367** | **0.607** | **0.576** | **0.572** |
| DMSP F16 | 0.619*** | 0.611*** | 0.587*** | 0.441*** | 0.330*** | 0.300*** |
| | (0.021) | (0.021) | (0.021) | (0.026) | (0.028) | (0.030) |
| **Adjusted $R^2$** | **0.377** | **0.369** | **0.351** | **0.610** | **0.576** | **0.566** |
| VIIRS Night Lights | 0.668*** | 0.629*** | 0.601*** | 0.478*** | 0.365*** | 0.339*** |
| | (0.020) | (0.020) | (0.021) | (0.024) | (0.027) | (0.029) |
| **Adjusted $R^2$** | **0.443** | **0.393** | **0.360** | **0.635** | **0.586** | **0.576** |
| Black Marble, weighted average | 0.711*** | 0.658*** | 0.517*** | 0.489*** | 0.396*** | 0.227*** |
| | (0.019) | (0.020) | (0.023) | (0.024) | (0.028) | (0.027) |
| **Adjusted $R^2$** | **0.502** | **0.430** | **0.266** | **0.634** | **0.591** | **0.557** |
| Black Marble, snow-free | 0.712*** | 0.659*** | 0.633*** | 0.476*** | 0.403*** | 0.379*** |
| | (0.019) | (0.020) | (0.020) | (0.024) | (0.028) | (0.030) |
| **Adjusted $R^2$** | **0.503** | **0.433** | **0.398** | **0.635** | **0.593** | **0.580** |
| Luojia-01 | 0.437*** | 0.548*** | 0.390*** | 0.211*** | 0.208*** | 0.131*** |
| | (0.024) | (0.022) | (0.024) | (0.020) | (0.024) | (0.021) |
| **Adjusted $R^2$** | **0.190** | **0.300** | **0.152** | **0.567** | **0.559** | **0.547** |

*Notes:* The dependent variable is the logarithm of fiscal revenue. Coefficients are for standardized variables to aid comparability across outcomes and specifications of NTL data. The sample is $n$=1460 rural counties. Robust standard errors in ( ), $^{***}$, $^{**}$, and $^{*}$ denote statistical significance at 1%, 5% and 10% levels. The control variables in columns (4) to (6) are elevation, precipitation, temperature, and five types of land cover (urban, village, industrial and infrastructural, cultivated land and forest ).